River Influences on Shelf Ecosystems: Introduction and Synthesis

Hickey[1], B.M. and R.M. Kudela[2], J.D. Nash[3], K.W. Bruland[2], W.T. Peterson[4], P. MacCready[1], E.J. Lessard[1], D.A. Jay[5], N.S. Banas[6], A.M. Baptista[7], E.P. Dever[3], P.M. Kosro[3], L.K. Kilcher[3], A.R. Horner-Devine[8], E.D. Zaron[5], R.M. McCabe[9], J.O. Peterson[3], P.M. Orton[10], J. Pan[5] and M.C. Lohan[11]

[1]School of Oceanography, University of Washington, Seattle, Washington, USA; bhickey@u.washington.edu

[2]Ocean Sciences and Institute for Marine Sciences, University of California, Santa Cruz, California, USA

[3]College of Ocean and Atmospheric Sciences, Oregon State University, Corvallis, Oregon, USA

[4] Northwest Fisheries Science Center, NOAA Fisheries, Newport, Oregon, USA

[5]Civil and Environmental Engineering, Portland State University, Portland, Oregon, USA

[6] Applied Physics Laboratory, University of Washington, Seattle, Washington, USA

[7] Science and Technology Center for Coastal Margin Observation and Prediction, Oregon Science and Health University, Beaverton, Oregon, USA

[8] Civil and Environmental Engineering, University of Washington, Seattle, Washington, USA

[9] University of New South Wales, Department of Aviation, Sydney, New South Wales, Australia

[10] Lamont-Doherty Earth Observatory, Columbia University, New York, New York, USA

[11] SEOS, University of Plymouth, Plymouth, PL48AA, England

Abstract

River Influences on Shelf Ecosystems (RISE) is the first comprehensive interdisciplinary study of the rates and dynamics governing the mixing of river and coastal waters in an eastern boundary current system, as well as the effects of the resultant plume on phytoplankton standing stocks, growth and grazing rates, and community structure. The RISE Special Volume presents initial RISE results deduced from four field studies and two different numerical model applications including an ecosystem model, on the buoyant plume originating from the Columbia River. This introductory paper provides background information on variability during RISE field efforts as well as a synthesis of results, with particular attention to the questions and hypotheses that motivated this research. RISE studies have shown that the maximum mixing of Columbia River and ocean water occurs primarily near plume lift-off inside the estuary and in the near field of the plume. Thus, most plume nitrate originates from upwelled shelf water, and plume phytoplankton species are typically the same as those found in the adjacent coastal ocean. River-supplied nitrate can help maintain the ecosystem during periods of delayed upwelling. The plume inhibits iron limitation, but

45 nitrate limitation is observed in aging plumes. The plume also has significant effects on
46 rates of primary productivity and growth (higher in new plume water) and
47 microzooplankton grazing (lower in the plume near field and north of the river mouth);
48 macrozooplankton concentration (enhanced at plume fronts); offshelf chlorophyll export;
49 as well as the development of a chlorophyll "shadow zone" off northern Oregon.

1. Introduction: The RISE Hypotheses

The coastal waters of the U.S. Pacific Northwest (PNW) house a rich and productive ecosystem. However, chlorophyll is not uniform in this region: it is typically greater in the Columbia River plume and over the coast north of the Columbia than south of the river mouth, as illustrated in Figure 1. This view is supported on a seasonal basis by time series of vertically integrated chlorophyll (Landry et al., 1989) and by satellite-derived ocean color (Strub et al., 1990; Thomas et al., 2001; Legaard and Thomas, 2006; Thomas and Weatherbee, 2006; Venegas et al., 2008). South of the Columbia, only over Heceta Bank does chlorophyll approach values as high as over the northern shelves (Fig. 1). The higher chlorophyll concentrations of the northern PNW coast are surprising because alongshore wind stress, presumed responsible for macronutrient supply in this Eastern Boundary upwelling system, increases southward over the California Current System (CCS) by a factor of eight (Hickey and Banas, 2003, 2008; Ware and Thomson, 2005). Greater productivity off the northern coast and near the Columbia plume has also been reported in higher trophic groups (e.g., euphausiids and copepods; Landry and Lorenzen, 1989). Juvenile salmon are more abundant north of the coast and in the plume (Pearcy, 1992; Bi et al., 2007).

In 2004 an interdisciplinary study "River Influences on Shelf Ecosystems" (RISE) was initiated to determine the extent to which alongshore gradients in ecosystem

productivity might be related to the existence of the massive freshwater plume from the Columbia River. RISE was designed to test three hypotheses:

- During upwelling the growth rate of phytoplankton within the Columbia plume exceeds that in nearby areas outside the plume being fueled by the same upwelling nitrate.
- The plume enhances cross-margin transport of plankton and nutrients.
- Plume-specific nutrients (Fe and Si) alter and enhance shelf productivity preferentially north of the river mouth.

RISE is the first comprehensive interdisciplinary study of the rates and dynamics governing the mixing of river and coastal waters in an eastern boundary system, as well as the effects of the buoyant plume formed by those processes on phytoplankton growth and grazing rates, standing stocks and community structure in the local ecosystem. This paper presents an overview of the project measurements and setting as well as a synthetic view of initial results. Background information on shelf processes, the Columbia River estuary and the Columbia River plume is presented in Section 2, followed by a description of the RISE sampling scheme and numerical models (Sec. 3). The environmental and biological setting of the RISE study years is given in Section 4. Study results as they pertain to plume-related questions and hypotheses are discussed in Section 5 and summarized in the last section.

2. Background

2.1 Shelf Processes Influencing the Columbia Plume

95 The buoyant plume from the Columbia River is located near the northern terminus of
96 an eastern boundary current. Water property, nutrients, biomass and current variability
97 are governed by wind-driven processes and dominated by the seasonal cycle. The
98 seasonal variability of physical, chemical and biological properties for both Oregon and
99 Washington are documented in Landry et al. (1989) and in the book edited by Landry and
100 Hickey (1989). In winter, large scale currents are primarily northward (the Davidson
101 Current); in summer, large scale currents are primarily southward (the California Current)
102 (Hickey, 1979, 1989, 1998). A coast-wide phenomenon that initiates the uplift of
103 isopycnals and associated higher nutrient and lower oxygen water from the continental
104 slope to the shelf, the "Spring Transition" (Huyer et al., 1979; Strub et al., 1987),
105 separates winter from the springtime growing season. Both the spring transition and the
106 seasonal continuation of upwelling through fall have been attributed in part to winds
107 south of the region (i.e., "remote forcing") (Strub et al., 1987; Hickey et al., 2006; Pierce
108 et al., 2006). The uplifted isopycnals result in the formation of a baroclinic coastal jet, a
109 feature which in mid summer is generally concentrated over the outer shelf and upper
110 slope off the coasts of northern Oregon (Kosro, 2005) and Washington (MacFadyen et
111 al., 2005).
112 Fluctuations in currents and water properties in this region occur on scales of 2–20
113 days throughout the year (Hickey, 1989). These fluctuations are driven in part by
114 fluctuations in local winds, and in part by coastally trapped waves generated by remote
115 winds (Battisti and Hickey, 1984). Although a change in wind direction from upwelling-
116 favorable (southward) to downwelling-favorable (northward) reverses the direction of
117 flow from southward to northward on the inner shelf where flow is frictionally dominated

118 (Hickey et al., 2005), surface currents on the outer shelf and slope rarely reverse (Kosro,
119 2005; MacFadyen et al., 2008). The stability of the shelf break jet is due primarily to its
120 baroclinic nature: reversals of wind stress to downwelling-favorable are insufficient to
121 completely erode the seasonally uplifted isopycnals during the upwelling season.
122 However, within a distance of about 10 km from the coast (the scale of the internal
123 Rossby radius of deformation), the response to changes in wind direction is almost
124 immediate (~3 hr, Hickey, 1989), resulting in significant vertical movement of isopycnals
125 on time scales of a few days. When winds are directed southward, the associated
126 upwelling of nutrient-rich water on the inner shelf fuels coastal productivity, resulting in
127 changes in chlorophyll concentration that follow the changes in wind direction. During an
128 upwelling event, phytoplankton begin to grow as a response to the infusion of nutrients
129 near the coast and this "bloom" is advected offshore, continuing to grow while depleting
130 the nutrient supply. When winds relax or reverse, the bloom moves back toward shore
131 where it can contact the coast and enter coastal estuaries (Roegner et al., 2002).
132 Although alongshelf currents do not typically reverse on the mid to outer shelf,
133 currents in the surface Ekman layer frequently reverse from onshore to offshore and vice
134 versa in response to southward or northward wind stress, respectively (Hickey et al.,
135 2005). Cross-shelf movement of buoyant plumes is particularly sensitive to wind stress
136 direction, because the Ekman layer is compressed by the plume stratification so that
137 velocities are correspondingly higher.
138 Water flowing south toward the Columbia plume region in summer has its source in a
139 topographically complex region offshore of the Strait of Juan de Fuca, which includes a
140 seasonal eddy (Fig. 2). Enhanced upwelling, in combination with outflow from the Strait,

141 makes this region a massive source of nutrients and chlorophyll for the shelf north of the
142 Columbia River (MacFadyen et al., 2008). Upwelled nitrate supplied to this region by
143 Strait related processes is about the same magnitude as that supplied to the entire
144 Washington coast over the upwelling season (Hickey and Banas, 2008). Moreover, the
145 elevated nitrate is distributed to greater distances offshore because of the Juan de Fuca
146 eddy, and to greater depths in the water column because of the Strait outflow, so that this
147 region is particularly rich in chlorophyll (Hickey and Banas, 2008). Water from this
148 region can transit the entire Washington shelf from north to south in a week or less under
149 strong upwelling conditions (MacFadyen et al., 2008).
150
151 2.2 The Columbia River Estuary
152 The Columbia estuary has been the subject of a number of physical oceanographic
153 studies (Hughes and Rattray, 1980; Giese and Jay, 1989; Hamilton, 1990; Jay and Smith,
154 1990a,b,c; Jay and Musiak, 1996; Cudaback and Jay, 2000, 2001; Kay and Jay, 2003a,b;
155 Orton and Jay, 2005; Chawla et al., 2008). The width of the estuary at its mouth is about
156 4 km and the depth over the bar is about 18 m. The ratio of the estuary width at the mouth
157 to the baroclinic Rossby radius near the mouth is typically about 0.2–0.4 (the Kelvin
158 number), so the estuary is considered dynamically narrow. The tidal prism (defined as the
159 integrated volume between mean lower low and high waters) varies from about half to
160 ten times the river flow volume. The density field within the estuary normally alternates
161 between two states—one, weakly stratified or partially mixed, which occurs during low-
162 flow periods with strong tides; the other, highly stratified (nearly salt wedge), which
163 occurs under most other conditions. Early interdisciplinary studies on the estuary and

plume were summarized in the book by Pruter and Alverson (1972). More recently, the Columbia estuary has been the focus of a Land Margin Ecosystem Research (LMER) program (Simenstad et al., 1990a). The estuarine ecosystem is supported largely by exogenous organic material supplied by the river, rather than by in situ primary production (Simenstad et al., 1990b; Sullivan et al., 2001; Small et al., 2001). Export of chlorophyll from the estuary to the plume is minimal, and occurs preferentially on spring tides before and after the spring freshet season (Fain et al., 2001; Sullivan et al., 2001).

2.3 The Columbia River Plume

The Columbia River accounts for 77% of the drainage along the U.S. West coast north of San Francisco (Barnes et al., 1972). The plume from the Columbia varies in volume from 2–11x10^{10} m^3, with maximum volume due to late spring snowmelt freshets and in winter due to rainfall (Hickey et al., 1998) and a seasonal minimum in late summer/early fall. Riverflow into the estuary varies from about 2.5–11x10^3 m^3 s^{-1} over a typical year (Bottom et al., 2005). Summertime river input into the other two coastal estuaries off the Washington coast is typically less than 1% of that from the Columbia River (Hickey and Banas, 2003). The Columbia River plume is more strongly forced at the estuary boundary than other US river systems, creating a spatially and temporally complex region near the river mouth. Because of the narrow outlet to the ocean, strong tidal currents and significant freshwater flow, surface currents in the tidal plume often exceed 3 m s^{-1} during strong ebb tides. As a result the Columbia River produces a highly supercritical outflow that propagates seaward as a gravity current during each ebb tide.

186 The leading-edge front, termed the "tidal plume front", produces strong horizontal
187 convergences, vertical velocities and mixing (Orton and Jay, 2005; Morgan et al., 2005).
188 The historical picture of the Columbia River plume depicts a low salinity feature
189 oriented southwest offshore of the Oregon shelf in summer (e.g., Fig. 1) and north or
190 northwest along the Washington shelf in winter (Barnes et al., 1972; Landry et al., 1989).
191 The RISE hypotheses were based on that view of the Columbia. Recently, Hickey et al.
192 (2005) have demonstrated that the plume can be present more than a hundred kilometers
193 north of the river mouth on the Washington shelf from spring to fall. This study showed
194 that the plume is frequently bi-directional, with simultaneous branches both north and
195 south of the river mouth. This spatial structure was subsequently confirmed by remote
196 sensing (Thomas and Weatherbee, 2006). During downwelling-favorable winds, the
197 southwest plume moves onshore over the Oregon shelf. At the same time, a new plume
198 forms north of the river mouth, trapped within ~20–30 km of the coast. This plume
199 propagates and also is advected northward by inner shelf currents that reverse during the
200 downwelling winds. When winds return to upwelling-favorable, inner shelf currents
201 reverse immediately to southward and the shallow plume is advected offshore in the
202 wind-driven Ekman layer to the central shelf, and southward in the seasonal mean
203 ambient flow (Hickey et al., 2005). The possibility of a bi-directional Columbia plume
204 depends critically on the existence of mean ambient flow in the direction opposite to its
205 rotational tendency. Because three out of four RISE cruises occurred early in the
206 upwelling season, most sampling took place in a bi-directional plume environment.
207 On subtidal timescales, numerical and laboratory models of river plume formation in
208 a rotating system under conditions of no applied winds and no ambient flow demonstrate

209 that a plume forms a non linear "bulge region" and a quasi-geostrophic "coastal current"
210 downstream of the bulge (e.g., Chao and Boicourt, 1986; Garvine, 1999; Yankovsky et
211 al., 2001; Fong and Geyer, 2002; Horner-Devine et al., 2006). Most of these prior studies
212 addressed the dynamics of uni-directional plumes over shallow broad shelves with low
213 riverflow, conditions typical for the US east coast. However the Columbia River
214 generates a large volume plume which emerges onto a relatively narrow continental shelf.
215 Perhaps its most unusual characteristic is that in summer it usually encounters ambient
216 flow moving counter to the rotational tendency of the plume. Prior to RISE, only the
217 model study by Garcia-Berdeal et al. (2002) addressed conditions applicable to the
218 Columbia. That study provided a dynamical basis for the existence of a bi-directional
219 plume and the time varying response of the plume to variable winds as well as to ambient
220 flow both in the same direction as, and counter to, the rotational tendency. The study also
221 demonstrated that over the shelf away from the river mouth, the effect of the plume on
222 the velocity field is confined to layers of low salinity (i.e., the plume effect is baroclinic),
223 as shown in a wintertime Columbia plume data set (Hickey et al., 1998).
224 With respect to nutrients, historical studies showed that in summer the Columbia
225 plume usually supplies exceptionally high concentrations of silicic acid (Si) but very little
226 nitrate, to the plume region (Conomos et al., 1972). Because sediment transport and
227 deposition from the Columbia plume is highest north of the river mouth (Nittrouer,
228 1978), that shelf potentially has a massive supply of Fe-rich sediment deposited on the
229 mid shelf region ready to be delivered to the euphotic zone by upwelling of bottom water
230 that has been in contact with the sediments. In addition, the broader, flatter shelf north of
231 the river mouth has been hypothesized to provide opportunity for increased duration of

bottom contact (hence access to Fe) of upwelling waters than the narrower, steeper shelf to the south (Bruland et al., 2001; Chase et al., 2007). The mid-shelf mud deposits can be thought to act like an iron capacitor; charging in the winter with the higher sediment transport associated with winter flood events, and discharging during the summer upwelling periods.

3. RISE Sampling Scheme and Modeling Systems

The overall RISE sampling strategy was to compare mixing rates, nutrient supply, and phytoplankton production, grazing and community structure within the plume and outside the plume; i.e., on the shelf north of the river mouth, presumed more productive, and on the shelf south of the river mouth, presumed less productive, as well as in the important "plume lift off" zone (the region where the plume loses contact with the bottom, located in the river entrance to ~5 km offshore of the entrance jetties). The backbone for this project consists of data collected during four cruises that took place in the seasonally high-flow period (May–June) in each of three years (2004–2006) and in a low-flow period in one year (August, 2005). The sampling was spread over three years to include potential interannual differences in processes related to wind and river flow variability. The 21-day length of the cruises ensured that a variety of circulation and growth regimes, including upwelling, relaxation/downwelling and neap/spring tides were observed.

254 The sampling plan as originally proposed was based on the historical picture of a
255 primarily southwest tending Columbia plume. However, due to the rarity of persistent
256 upwelling-favorable winds on RISE cruises, southwest-tending plumes were the
257 exception rather than the rule. In particular, on two of the cruises, June 2005 and May–
258 June 2006, north-tending plumes were dominant: RISE sampling was adapted to this
259 situation, and samples were obtained along the Washington coast as far north as the Strait
260 of Juan de Fuca in 2006.
261 The field studies used two vessels operating simultaneously. The R/V Wecoma
262 obtained primarily biological and chemical rate data: a) at individual stations on cardinal
263 transects north and south of the river mouth (Grays Harbor and Cape Meares; see Fig. 2)
264 and near the river mouth; b) at selected process study stations; and c) at fixed stations
265 near the river mouth during strong neap and spring tides (time series). A towed sensor
266 package was used to obtain micronutrient samples near the sea surface on cardinal
267 transects and selected other transects. Underway measurements included macronutrients
268 (N, P, Si), dissolved trace metals (Fe, Mn), supplemented with discrete samples from the
269 underway system (microscopy, FlowCAM and particulate trace metals) as well as ADCP
270 (75 kHz) measurements of velocity. At CTD stations vertical profiles (0–200 m where
271 possible; and 500 m at selected stations) of T, S, currents, dissolved O_2, in vivo
272 fluorescence, transmissivity, PAR, and bottle samples for chlorophyll *a*, dissolved
273 macronutrients (NO_3, NH_4, urea, PO_4, SiO_4), dissolved trace metals, and heterotrophic
274 and autotrophic plankton composition were obtained. In addition, primary production
275 measurements were made each day at noon, and phytoplankton growth and
276 microzooplankton grazing measurements were made every one to two days.

Macrozooplankton were sampled with vertically towed nets and obliquely towed Bongo nets at selected stations; macrozooplankton experimental work included egg production rates of copepods and euphausiids and molting rates of euphausiids, to obtain estimates of secondary production. Surface drifters were used to follow the mixing of individual plumes from the Columbia and to provide information on surface currents.

On the R/V Point Sur, synoptic mesoscale and fine-scale features were sampled with underway measurements of near-surface T, S, velocity, particle size and concentration, PAR, transmissivity, fluorescence, and nitrate + nitrite. The Point Sur's Triaxus tow fish provided high-resolution sections of T, S, zooplankton (Laser-OPC), PAR and transmissivity, fluorescence, particle size and concentration (LISST-100), UV absorption and nitrate (Satlantic ISUS), upward-looking ADCP velocity (1200 kHz), and radiance/irradiance (7 channels) through the upper water column to 30–35 m. Rapidly executed transects of turbulence and fine-structure were also carried out using the Chameleon profiler; these provide full-depth profiles of T, S, optics (880 nm backscatter and fluorescence), turbulence dissipation rates and turbulent fluxes every 1–3 minutes. During selected periods, transects (primarily those identified in Figure 2) were repeated hourly to capture the high-frequency evolution in the plume's near-field and river estuary. Over-the-side deployed acoustics (1200 kHz ADCP and 120 kHz echosounder; 1-m nominal depth) augmented the hull-mounted 75 and 300 kHz units to image fine-scale features of the velocity and backscatter fields, resolving fronts, nonlinear internal waves, and turbulent billows.

The temporal context for observed variability was provided by an array of moored sensors deployed in the plume near field as well as on the shelf north and south of the

300 plume (Fig. 2), complemented by the pre-existing long-term estuarine and plume stations
301 of the CORIE/SATURN network (Baptista, 2006). To better resolve regional differences,
302 RISE moorings were moved farther north and south to the cardinal sampling transects
303 after the first year of the program (Fig. 2). Surface currents were mapped hourly from
304 shore using HF radar with two simultaneously operating arrays, one with a 40 km range
305 and a 2 km range resolution, the other with a 150 km range and a 6 km range resolution.
306 Satellite ocean color, sea surface temperature, turbidity and synthetic aperture radar
307 (SAR) were also obtained when available.

308 Two modeling systems were developed or enhanced during RISE. The system
309 developed specifically for RISE employed a structured grid model (ROMS) and was used
310 in hindcast mode (MacCready et al., 2009). The CORIE/SATURN modeling system
311 (Baptista, 2006), based on two unstructured-grid models (SELFE, Zhang and Baptista,
312 2008; and ELCIRC, Zhang et al., 2004), was used in both near real-time prognostic mode
313 (e.g., Zhang et al., 2009) and multi-year hindcast mode (e.g., Burla et al., 2009). Both
314 modeling systems incorporated the estuary in the simulation domain (although at
315 different resolutions) and used realistic atmospheric, river and ocean forcing including
316 tides. Wind/heat flux model forcing for ROMS was derived from the 4 km MM5 regional
317 wind/heat flux model (Mass et al., 2003). SELFE and ELCIRC were also forced by
318 MM5. Conditions on open boundaries were provided by Naval Research Laboratory
319 (NRL) models; ROMS used the smaller domain, higher resolution (~ 9 km) NCOM-CCS
320 NRL model (Shulman et al., 2004), SELFE and ELCIRC used the larger domain, lower
321 resolution (~16 km) global NCOM model (Barron et al., 2006). These models have
322 proven more effective in this region than climatology because they assimilate satellite

altimetry and sea surface temperature, thus ensuring the reasonable development of a southward coastal jet, inclusion of low mode coastal trapped waves that are a significant part of the mid shelf subtidal scale variance in this region (Battisti and Hickey, 1984). Both models became integral tools for planning and/or analysis within RISE.

The ROMS model was also used for biologically-motivated particle-tracking studies (Banas et al., 2009a) and ecosystem modeling (Banas et al., 2009b). The biological model is a four-box ("NPZD") nitrogen-budget model that tracks nutrients, phytoplankton, microzooplankton, and detritus in every cell of the ROMS grid. The rich RISE biological dataset allowed direct model validation against not just stocks (chlorophyll, microzooplankton, nutrients) but rates (phytoplankton growth and microzooplankton grazing), a level of validation that is seldom possible. Rate observations also allowed key model parameters (e.g., microzooplankton ingestion rate and mortality) to be prescribed empirically (Banas et al., 2009b).

During the RISE field years, another interdisciplinary program took place along the northern Washington, southern British Columbia coast. This project (Ecology of Harmful Algal Blooms Pacific Northwest, "ECOHAB PNW"), with a scientific team and suite of measurements similar to that of RISE, focused on the development of blooms of toxigenic *Pseudo-nitzschia* in the Juan de Fuca eddy region (see Fig. 2) and their subsequent transport to the Washington coast. Surveys were made as far south as offshore of Willapa Bay, and as far north as central Vancouver Island. Both RISE and ECOHAB PNW sampled a line off Grays Harbor, and the combined data were used in several papers in this and previous volumes (Hickey et al., 2006; Kudela et al., 2006; Frame and

345 Lessard, 2009). Data from the moored arrays in the two programs (see locations in Figure
346 2) have also been used together in papers for this volume (Hickey et al., 2009).
347
348 4. The RISE Years: Environmental and Biological Setting
349
350 Time series of the two commonly used indices for interannual variability, the
351 Multivariate El Niño Index (MEI) and the Pacific Decadal Oscillation (PDO) illustrate
352 that RISE studies all took place within periods when both indices were generally positive
353 (Fig. 3). Columbia and Willamette River (a major lower-basin Columbia River tributary)
354 flows are lowest in years when the PDO is positive (with a warm coastal ocean in the
355 Pacific Northwest) and the MEI index is positive (indicating El Niño-like conditions).
356 Average flows are about 20% lower than in La Niña years when the PDO is negative
357 (Dracup and Kahya, 1994; Gershunov et al., 1999; Bottom et al., 2005). Indeed, riverflow
358 was below average in spring of all RISE years except during a brief period in late May
359 2005 and from April though June 2006 (Fig. 4a). In May 2005, flow in the Willamette
360 River was unusually high (up to 200% of normal), leading to above average export of
361 nutrients from the estuary to the plume. Compared to historical records, nitrate was about
362 a factor of two higher in spring of both 2005 and 2006 in the Columbia River outflow, in
363 large part due to additional nutrient sources from coastal and valley rivers, in particular,
364 those that have been recently logged (Bruland et al., 2008).
365 Warmer than average surface waters were observed in the Pacific Northwest during
366 the RISE summers (Shaw et al., 2009), consistent with the occurrence of positive phases
367 of MEI and PDO. The fact that the warmer water is related to advection rather than local

368 heating is confirmed with time series of copepod species assemblages (Fig. 5). In an
369 average year, during winter months the northward-flowing Davidson Current transports
370 warm water "neritic" species (species restricted to coastal shelf environments) northward
371 from California to the Oregon and Washington shelves; during the upwelling season, cold
372 water species usually dominate and these species are transported southward from coastal
373 British Columbia and the coastal Gulf of Alaska. During the RISE project summers of
374 2003 through 2005 the copepod community was dominated by "warm water neritic"
375 species, as typically occurs when the PDO is positive (Hooff and Peterson, 2006). The
376 community began to transition to a cold water species phase during the summer of 2006,
377 consistent with the decreasing PDO (Fig. 3); however "warm water oceanic" species were
378 still conspicuous in samples. The figure also shows that during strong El Niño events (as
379 in late1997–1998) the copepod community is also dominated entirely by warm water
380 species (for both neritic and oceanic species). Thus, the RISE years were similar in some
381 respects —biological (zooplankton) and physical (riverflow and surface water
382 temperatures) to El Niño conditions.
383 In spite of the low overall riverflow and El Niño-like conditions, short term
384 variability in physical and biological conditions in this region is sufficiently strong that
385 conditions of both high and low riverflow, upwelling and downwelling occurred and
386 were sampled during the RISE cruises. The RISE 1 cruise in July 2004 took place in a
387 year with the lowest riverflow observed on RISE cruises (Fig. 4a). The cruise included a
388 period of persistent upwelling winds and, perhaps more significant, the largest southward
389 flows sampled during the RISE cruises (Fig. 6). A well developed southwest tending
390 plume was observed, and samples were taken along its axis. Nitrate was supplied to the

391 plume via upwelled nitrate-rich waters mixing with nitrate-depleted river water during
392 plume formation (Bruland et al., 2008). Seasonal upwelling prior to the cruise was the
393 weakest observed during RISE years (Fig. 4b).
394 In 2005, upwelling over the inner shelf was delayed (Hickey et al., 2006; Kosro et al.,
395 2006) and the May–June RISE 2 cruise took place prior to the onset of strong upwelling-
396 favorable winds and just after a period of higher-than-average riverflow (Figs. 4b and 6).
397 A weak southwest tending plume was observed at the beginning of the cruise, but most
398 cruise sampling took place in a northward tending plume. Plume nutrients were being
399 supplied from the watershed rather than from the coastal ocean (Bruland et al., 2008),
400 resulting in substantially lower than expected coastal productivity (Kudela et al., 2006).
401 RISE 3 took place in August 2005 in a period with the lowest riverflow of all the
402 RISE cruises (Fig. 4a) and after upwelling winds had become persistent (Figs. 4b and 6).
403 A strong well-developed southwest plume was observed and sampled. This was the only
404 observation of actual upwelling off the Washington coast in all of the RISE cruises.
405 Plume nutrients were being provided from upwelling water that mixed with the
406 outflowing riverflow (Bruland et al., 2008).
407 The final RISE cruise took place in May–early June 2006 under extremely high
408 riverflow conditions, the highest observed in the four RISE cruises (Fig. 4a).
409 Downwelling-favorable winds were also higher than typically observed at that time of
410 year as indicated by the significant dip in the cumulative wind stress curve during the
411 cruise period (Figs. 4b and 6). The majority of the cruise time was used sampling north-
412 tending plumes, following the plumes as far north as the Strait of Juan de Fuca (Hickey et
413 al., 2009). However, a new southwest-tending plume developed during the last few days

414 of the cruise. In that period, the river itself was supplying plume nutrients to both north-
415 and southwest-tending plumes (Bruland et al., 2008). Surface drifters were used to follow
416 the newly emerging southwest plume, sampling its chemical and biological aging with
417 cross-plume transects (Hickey et al., 2009).
418
419 5. RISE Results
420
421 Several key issues on the development, evolution and importance of river plumes to
422 the regional ecosystem remained at the outset of RISE. One of the least understood
423 phenomena with respect to river plumes was how the freshwater discharge mixes with
424 ambient coastal waters (Boicourt et al., 1998; Wiseman and Garvine, 1995). Another
425 important issue was the effect of a buoyant plume on local transport pathways. A third
426 critical issue was captured by the overall RISE question: how does a buoyant plume
427 impact the ecosystem? The results of RISE as they pertain to these important issues, as
428 well as our ability to model these processes and impacts are summarized below.
429
430 5.1 Regional Plume Effects
431 a) *Does the plume alter phytoplankton growth rates, grazing rates or species*
432 *composition in comparison to active upwelling regions?*
433 A trend towards higher biomass of phytoplankton on the Washington versus Oregon
434 shelf has been attributed to increased retention due to shelf width and/or forcing time as
435 well as effects of freshwater (Hickey and Banas, 2003, 2008; Ware and Thomson, 2005),
436 enhanced nitrate supply (Hickey and Banas, 2008) and iron availability (Lohan and

437 Bruland, 2006; Chase et al., 2007). Chlorophyll data taken on near-simultaneous RISE
438 sections off Washington and central Oregon are consistent with this pattern (Fig. 7a):
439 chlorophyll concentrations are almost always higher toward the north. Chlorophyll data
440 from selected biological process stations averaged over each cruise are also consistent
441 with the general trend of higher chlorophyll to the north, although the difference is not
442 significant (Frame and Lessard, 2009). The data in Figure 7a were derived from
443 regression between CTD fluorescence and measured chlorophyll (r^2 ~0.72–0.77 for the
444 four cruises). However, even isolated extrema such as on May 22, 2006 on the GH
445 transect were very similar to the bottle-derived surface Chl values. Surface concentrations
446 were higher to the south at stations close to the coast in the two periods when upwelling
447 was occurring (July 2004 and August 2005), consistent with the tendency for stronger
448 and earlier upwelling off Oregon. The surface cross shelf chlorophyll structure along the
449 GH and CM transects on July 24–25, 2004 in Figure 7a is very similar to that shown in
450 the satellite image of July 23, 2004 (Fig. 1): the higher surface chlorophyll extending
451 across much of the shelf off Grays Harbor is reflective of the higher surface chlorophyll
452 along most of the Washington/southern British Columbia coast. This feature terminates
453 just south of the Columbia plume region and consequently is not observed off Cape
454 Meares.

455 In RISE, we addressed the role of the Columbia River plume on phytoplankton
456 growth, grazing and physiology using a number of empirical and modeling approaches.
457 We directly compared phytoplankton intrinsic growth and grazing rates (Lessard and
458 Frame, 2008; Lessard et al., in prep.) in over 100 dilution experiments as well as plankton
459 community composition (Frame and Lessard, 2009) within the plume and on the

460 Washington and Oregon shelves. Phytoplankton intrinsic growth rates were not different
461 on the Washington and Oregon shelves, but were significantly higher in the near-field
462 Columbia plume region. Grazing pressure (grazing:growth ratio) was lowest in the near-
463 field plume and highest off Oregon (Frame and Lessard, 2009).

464 Diatoms dominated the phytoplankton biomass in most samples, and diatom
465 community composition was very similar on both shelves within a cruise; there was no
466 strong evidence for a unique phytoplankton assemblage within the plume (Frame and
467 Lessard, 2009). Nevertheless, when assemblages inside and outside plumes were
468 compared for individual plume events, differences in community composition were
469 sometimes observed. For example, samples closely spaced in time during a southwest
470 plume event in August 2005 and also a north plume event in spring 2006 had different
471 non-diatom communities in the plume and outside the plume; and a southwest plume in
472 spring 2006 had different diatom communities inside and outside the plume (Frame and
473 Lessard, 2009).

474 Phytoplankton net growth and chlorophyll size-fractions were examined in a series of
475 multi-day deckboard incubations with added nutrients or filtered plume water in summer
476 2005 (Kudela and Peterson, 2009). There was no evidence for an inherent physiological
477 difference in phytoplankton assemblages between the Oregon and Washington shelf
478 waters adjacent to the Columbia River plume, nor was there evidence for short-term
479 effects of iron limitation or enhancement by other constituents of the plume water (e.g.,
480 Zn, organic matter). However, Frame and Lessard (2009) noted that in spring 2006, after
481 an earlier strong upwelling event and intense diatom bloom, the coastal water outside the

plume had residual nitrate and was dominated by small cells (cyanobacteria and picoeukaryotes), which was consistent with possible iron limitation at that time.

The alongshore difference in grazing pressure (higher off Oregon than off Washington) likely plays a significant role in maintaining higher chlorophyll concentrations on the Washington shelf (Lessard and Frame, 2008; Lessard et al., in prep.). In addition, model results show that the plume forms a "barrier" to biomass transport to Oregon, deflecting up to 20% of the phytoplankton biomass offshore (see below) (Banas et al., 2009b). The wider shelf north of the Columbia (affecting retention patterns and possible bloom spin-up times) as well as the retentive characteristics of the Juan de Fuca eddy that feeds the Washington shelf from the north also play important roles in producing alongcoast spatial gradients (Hickey and Banas, 2008).

With respect to macrozooplankton, RISE investigators studied egg production and molting rates of two copepod species (*Calanus marshallae* and *C. pacificus*) and two euphausiid species (*Euphausia pacifica* and *Thysanoessa spinifera*) on the shelves north and south of the plume (Shaw et al., 2009). *E. pacifica* growth rates were significantly higher during June 2006 versus July 2004 and June 2005, but not significantly different between the RISE study area and stations off Newport, Oregon. Euphausiid brood sizes were significantly higher during August 2005 versus any of the other cruises for both *E. pacifica* and *Thysanoessa spinifera*, but again there was no indication that brood sizes were higher in the northern part of the RISE study region. Significant differences in egg production rates (EPRs) were found among cruises for both *Calanus pacificus* and *C. marshallae*, with higher EPRs during August 2005, the only cruise with substantial amounts of upwelling. EPRs were low on other cruises, less than half the maximum rates

505 known for these species. Overall, the interannual differences in oceanographic conditions
506 during this study seemed to affect zooplankton production more strongly than the
507 hypothesized differences with latitude. The authors caution, however, that growth rate
508 and brood size are not necessarily good proxies for standing stocks. Because no
509 difference in Euphausiid egg production rates was observed between regions, we are left
510 with the alternate hypothesis that there is a higher biomass of euphausiids off the
511 Washington coast due to the influence of submarine canyons on zooplankton, as
512 suggested by Swartzman and Hickey (2003).
513
514 b) *Does the plume enhance either export or retention of regional biomass on the*
515 *shelf?*
516 Particle-tracking analysis in the MacCready et al. (2009) circulation model
517 demonstrates that the plume disperses water in multiple directions under variable winds
518 (Banas et al., 2009a). Washington coastal water moves farther north under northward
519 winds when the plume is included in the model, compared with a model scenario in
520 which it is omitted; during some transient conditions coastal water is advected farther
521 south under southward winds as well; and, most significant, coastal water is episodically
522 shifted seaward by plume effects. The mechanisms are a combination of increased
523 entrainment into transient topographic eddies driven by wind intermittency; creation of
524 additional eddies through tidal pulsing (Horner-Devine et al., 2009); shear between the
525 anticyclonic bulge circulation and ambient southward flow (Yankovsky et al., 2001;
526 Garcia-Berdeal et al., 2002); and enhanced offshore flow in the surface Ekman layer of
527 the plume, which is vertically compressed by the plume stratification. The net effect of

528 these processes during a model hindcast of July 2004 was to export 25% more water from
529 the Washington inner shelf past the 100 m isobath, when the plume was included in the
530 model versus when it was not (Banas et al., 2009a).

531 This net export of water is reflected in a seaward shift in biomass and primary
532 production in the Banas et al. (2009b) biophysical model as well. Inclusion of the plume
533 was found to decrease primary production on the inner shelf by 20% under weak-to-
534 moderate upwelling winds, and simultaneously to increase primary production on the
535 outer shelf and slope by 10-20%. This seaward shift mainly reflects a shift in biomass
536 distribution, rather than a shift in growth rates or spatially-integrated production.

537 Empirical data of macro-zooplankton-sized particle distribution and chlorophyll
538 fluorescence from the May 2005 survey (Figure 1 in Peterson and Peterson, 2008) are
539 consistent with the model results: maximum zooplankton abundance and chlorophyll
540 fluorescence follow the path of the southward flowing plume. North of the plume,
541 maximum values occur between the 50 and 100 m isobath. South of the river mouth, the
542 maxima are shifted offshore, extending to the outer shelf and slope. With the available
543 data, however, localized growth and aggregation cannot be distinguished from advective
544 processes. In proximity to the river mouth, aggregations of zooplankton can be pushed
545 across the shelf at velocities up to 38 cm s^{-1}, roughly 5-fold faster than typical wind-
546 driven Ekman transport in the region (Peterson and Peterson, 2009).

547 Under some conditions, the plume can also enhance retention of water and biomass
548 (Hickey and Banas, 2008). For example, on the inner shelf north of the river mouth
549 retention typically occurs after a well developed north-tending plume that was formed
550 during a period of downwelling winds moves away from the coast during a subsequent

551 period of upwelling winds: the shoreward plume front forms a barrier to cross-shelf
552 transport. Model studies also suggest (Banas et al., 2009a, 2009b) that interactions
553 between the plume and variable winds episodically retard the equatorward advection of
554 biomass from the Washington shelf, so that the plume acts as a retention feature in an
555 alongcoast sense as well (Hickey and Banas, 2008).
556
557 c) *Does the plume spatially concentrate plankton? If so, where?*
558 Broad-scale and fine-scale surveys with a Triaxus tow-body equipped with a Laser
559 Optical Plankton Counter and CTD provided a detailed picture of the relationship
560 between plume waters and macrozooplankton-sized particle distributions. Overall,
561 vertically-integrated zooplankton-sized particle abundance and biovolume were elevated
562 in proximity to "aged" plume waters (i.e., surface salinity between 25 and 30). Integrated
563 abundance was approximately 7×10^6 particles m^{-2} in proximity to "aged" plume waters,
564 and 4×10^6 particles m^{-2} outside these areas. In addition, zooplankton tended to aggregate
565 near the surface (upper 10 m) in proximity to river plume waters and were deeper in the
566 water column (25 m) when the plume was not present (Peterson and Peterson, 2009).
567 Analysis of the evolution of salinity following drifters released at the estuary mouth
568 during maximum ebb shows that surface waters overtake the plume front (McCabe et al.,
569 2008, 2009), clearly indicating that the front is a surface convergence feature. Fine-scale
570 surveys across the plume front revealed that during a strong ebb-tide, zooplankton-sized
571 particles were up to 2-fold more concentrated on the seaward side of the plume front
572 compared to concentrations 3 km on either side of the front (Peterson and Peterson,
573 2009). Physical processes associated with the developing plume vertically depressed

574 dense layers of phytoplankton and zooplankton an average of 7 m deeper into the water
575 column both beneath the plume and up to 10 km seaward of the plume front; this feature
576 may be associated with plume-related nonlinear internal waves (see Sec. 5.3c).
577
578 d) *Do nutrients supplied by the plume enhance productivity on a regional basis?*
579 Nitrate and other nutrients are upwelled onto the shelf seasonally. Upwelling-
580 favorable wind stress decreases northward by about a factor of two over the RISE region.
581 RISE nitrate data illustrate that in spite of this decline, nitrate concentrations below the
582 surface layer (~20 m) across the shelf are as high or higher toward the north in the RISE
583 region (Fig. 7b). In the upper water column, alongcoast nitrate can be higher to the north
584 or to the south, due to biological drawdown (Fig. 7b).
585 During strong upwelling periods when the Columbia River plume is directed
586 southwest off the Oregon shelf, upwelled nitrate from the shelf mixed into the plume in
587 the estuary and near the river mouth is the dominant source of nutrients in the plume.
588 During periods of downwelling, when isopycnals and associated high values of nitrate
589 move downward and offshore, this supply route is eliminated. Unlike the Mississippi
590 River, nitrate supply to the plume from its watershed is low in summer (Conomos et al.,
591 1972; Sullivan et al., 2001). However, in some spring periods, particularly when rainfall
592 is higher than normal, elevated nitrate concentrations from the watershed can be
593 delivered to the ocean by the high riverflow (Bruland et al., 2008). A seasonal nitrate
594 budget for this region suggests that nitrate input from the Columbia watersheds is two
595 orders of magnitude smaller than input from coastal upwelling, from the Strait of Juan de
596 Fuca or from submarine canyons (Hickey and Banas, 2008). Although small in

597 comparison to other sources on a summer-averaged basis, watershed-derived nutrients
598 may help sustain the ecosystem during periods of delayed seasonal upwelling, as
599 occurred in 2005 (Hickey and Banas, 2008) and also during periods of downwelling.
600 Thus, whereas nitrate supply on the Oregon coast is shut off during downwelling or weak
601 winds, the Washington coast has an additional supply from the Columbia River to help
602 maintain productivity during such periods.
603 Recent measurements indicate that whereas iron can be a limiting nutrient off
604 California (Hutchins and Bruland, 1998; Hutchins et al., 1998; Bruland et al., 2001;
605 Firme et al., 2003), phytoplankton growth has not been observed to be iron limited off the
606 Oregon coast (Chase et al., 2002). RISE studies have shown that iron is not generally
607 limiting on the Washington coast (Kudela and Peterson, 2009; Lohan and Bruland, 2006,
608 2008; Bruland et al., 2008). Not only is the plume from the Columbia heavily laden with
609 iron, particulate iron from the Columbia plume is also deposited in mid-shelf sediments
610 along both the Washington and Oregon coasts. The iron-laden shelf sediment can be
611 mixed into bottom water and thus added to the already nitrate-rich water during coastal
612 upwelling (Lohan and Bruland, 2008).
613 A model study comparing results with and without a river plume has shown that more
614 nitrate is provided to the sea surface, and more biomass accumulates in the region near
615 the river mouth when the river plume is present (Hickey and Banas, 2008). The
616 enhancement is due not to the river itself, but to enhanced mixing by the large tidal
617 currents near the river mouth. Similar effects were seen just offshore of Washington's
618 other two other coastal estuaries.
619

e) *Does phytoplankton size differ between shelves north and south of the river mouth?*

On three of four RISE cruises size fractionated chlorophyll was measured at >20 μm and total (GF/F; nominally 0.7 μm) sizes. In the RISE region, the >20 μm size fraction is nearly completely dominated by diatoms (Frame and Lessard, 2009; Kudela et al., 2006). The percent >20 μm versus distance offshore on the cardinal transects off Washington and Oregon occupied within 1–2 days of each other is shown in Figure 8a. The presence or absence of a Columbia plume on these transects is indicated with a gray contour on chlorophyll and nitrate sections in Figures 7a,b. The left hand panels in Figure 8a illustrate cross-shelf structure during periods when the Columbia plume was observed on both transects; the right hand panels illustrate structure during periods of upwelling, although a plume is present off Oregon (CM transect) during May–June 2006.

Comparison between transects sampled at the start and end of the cruise in May–June 2005 (left panels) indicates significant temporal variability over periods of 10–15 days. On that cruise, the percent of large cells within 325 km of the Washington coast (CM transect) decreased significantly from 60–90% to 25–40% over the 2–3 week period between repeat transect sampling.

Significant spatial differences were observed between Washington and Oregon within 20–30 km of the coast during periods when the Columbia plume was present. In particular, the percent of large cells was smaller off the Washington coast (GH) at most stations (left panels, Fig. 8a). In contrast, during periods when upwelling had recently occurred or was active, the percent of large cells was similar off the two coasts (right panels, Fig. 8a). A two-tail student's t-test (assuming unequal variances) applied on all

643 data closer than 25 km from shore, for all four cruises and both Washington (GH) and
644 Oregon (CM) transects (n=16 and n=17 for >20 and >5 μm, respectively) gave p=0.001
645 and p=0.018 for the 20 and 5 μm size ranges, respectively, with the percent of large cells
646 higher off Oregon. This is a very conservative test, indicating that the results are highly
647 significant.

648 Figure 8a also shows that although cell size frequently decreases from nearshore to
649 offshore (Kudela et al., 2006), this pattern was altered in the presence of a plume: cell
650 size appears to increase with distance offshore on the GH transect (upper left panel). This
651 phenomenon is depicted explicitly in Figure 8b, where percent >20 μm is plotted against
652 salinity for the May–June 2005 cruise, during which the plume was observed on all
653 transects. The percent of large cells increases significantly with salinity following the
654 plume as it becomes saltier (i.e., "aging") on the first occupations of both Washington
655 (GH) and Oregon (CM) transects, with higher percents of large cells off Oregon. On the
656 second occupations of these transects, high salinity water (S >31 psu) appeared on the
657 offshore ends of sections (likely originating in the Strait of Juan de Fuca; MacFadyen et
658 al., 2008). These waters were clearly dominated by smaller cells, and the dilution with
659 this new water masked the increase in cells size with aging Columbia plume water in the
660 regression. Based on these data, it appears that size structure is more affected by physical
661 processes (upwelling and plume formation) than by latitude.
662
663 f) *Does turbidity influence phytoplankton photosynthesis?*
664 In contrast to expectations, there was not a strong response in phytoplankton
665 photosynthesis versus irradiance (PE) kinetics from stations within the plume. PE curves

collected from near-surface (2 m) and near-bottom in the near-field plume were generally indistinguishable from each other (ANCOVA; $p>0.05$), with more variability from consecutive ebb pulses (temporal variability) than with depth (Kudela, unpublished). In fact, within each cruise, there was a significantly positive relationship between increasing turbidity and increasing maximal chlorophyll-normalized productivity (Fig. 9). There is also a negative correlation of light transmission with both iron and nitrate concentrations, suggesting that the effects of turbidity on carbon assimilation were either not significant, or were overcome by the co-occurring increase in nutrients. During August 2005 (Fig. 9) ambient nitrate was in excess of the measured half-saturation parameter for nitrate uptake (Ks) for 5 of 7 PE curves (Kudela and Peterson, 2009), while the remaining two stations exhibited elevated carbon assimilation and turbidity (i.e., opposite expectations if the trend is a function of nitrate concentration), suggesting that plume turbidity does not have a negative impact on photosynthesis. Multi-day deckboard incubations during August 2005 also showed no evidence for iron limitation either within or outside the plume (Kudela and Peterson, 2009). Similar results have been reported for plumes in Lake Michigan, where Lohrenz et al. (2004) reported no effect on phytoplankton production inside and outside a persistent turbidity plume. Both the Lake Michigan and Columbia River plumes are dominated by particle scattering rather than absorption (e.g., due to colored dissolved material); this appears to result in a high turbidity, diffuse light environment that has relatively little impact on photosynthesizing organisms.

g) *What is the origin of plume turbidity in spring and summer?*

688 Detailed measurements of sediment fluxes into and out of the plume in the near-field
689 region highlight an important seasonal trend in the origin of sediment entering the plume
690 (Spahn et al., 2009). During the spring freshet of May 2006, delivery of sediment to the
691 plume from the river was relatively high and strong vertical stratification prevented
692 sediment from the seabed in the near-field region from entering the plume directly. In
693 contrast, data from the end of the summer in August 2005 show a decrease of input from
694 the river. Under these low-flow conditions the near-field plume is much less stratified and
695 strongly interacts with the bottom, generating bottom-attached fronts characterized by
696 elevated turbulence and vertical velocity, which carry re-suspended sediment from the
697 seabed towards the surface plume waters. Thus, the data suggest that sediments entering
698 the plume originate primarily from the river in spring and increasingly from the seabed
699 through the summer. This result is consistent with dissolved and labile particulate iron
700 measurements in August 2005 and May 2006, which also show a shift from fluvial to
701 marine sources over the course of the summer (Bruland et al., 2008; Lippiatt et al., 2009).
702
703 5.2 Regional Plume Structure and Modeling
704 a) *What is the spatial and temporal extent of the plume in spring/summer?*
705 Three major advancements in our understanding of Columbia plume extent, location
706 and structure were made during RISE. First it was demonstrated that in spring, under
707 conditions of high riverflow and strong northward winds, the Columbia can extend the
708 entire length of the Washington coast (~250 km), and then enter the Strait of Juan de
709 Fuca (Hickey et al., 2009). More important, the plume can interact directly with outflow
710 from the strait, and with the seasonal eddy associated with the strait outflow and the shelf

711 break jet. The Columbia plume water becomes entrained in this eddy, subsequently
712 returning southward toward the Columbia mouth, thus extending the residence time of
713 plume water over the shelf by several weeks. A second major finding is that southwest
714 tending plumes often seen in satellite images during upwelling-favorable wind conditions
715 can consist primarily of aged water that has spent days or even weeks on the Washington
716 shelf (Hickey et al., 2009; Liu et al., 2009a). Overall, RISE has shown that the spatial and
717 temporal influence of the plume on the shelf north of the river mouth in spring and
718 summer is much greater than expected from prior data and historical concepts.
719 A third advance was that RISE has provided a better conceptual view of the structure
720 of the plume. Garvine (1982) defined three plume components: the lift-off or source
721 zone, the near-field and the far-field. As described below, the strongly supercritical,
722 initial advance of the plume has resulted in the need to define new plume water on each
723 tide, bounded by a supercritical front, as the "tidal plume", distinct from the near-field
724 plume (Horner-Devine et al., 2009).
725
726 b) *How well can we model plume structure and variability?*
727 The two RISE circulation modeling systems attempt to give realistic simulations of
728 circulation both within the estuary and in the coastal ocean. In spite of this range of
729 scales, and while they differ in details from each other and observations, both modeling
730 systems provide useful insights into circulation dynamics and its response to external
731 forcing (Liu et al., 2009a,b; MacCready et al., 2009; Zhang et al., 2009; Burla et al.,
732 2009). In particular, both models capture changes in plume location, direction and size in
733 response to changes in river discharge and shelf winds. In addition, one of the modeling

734 systems (Baptista, 2006) offers real-time estuary and plume prediction in support of
735 cruises (Zhang et al., 2009), and the opportunity for decadal scale analysis of variability
736 (Burla et al., 2009). Neither model was designed to capture details of the nonhydrostatic
737 tidal plume front and the nonlinear internal waves that develop there (Nash and Moum,
738 2005; Kilcher et al., 2009).

739 The ROMS model uses a horizontal resolution of about 400 m in the estuary and
740 plume region, stretching to about 7 km at the far oceanic edges of the domain. Model
741 fields for the summer of 2004 were compared quantitatively with time series from the 3
742 RISE moorings, 5 CTD sections, HF Radar surface velocity, several tide stations, and a
743 number of moored instruments located within the estuary (maintained by the
744 CORIE/SATURN system). Overall the model data comparison was reasonably good
745 (MacCready et al., 2009; Liu et al., 2009b) with average model skill scores around 0.65,
746 comparable to that of the few other similar studies. Model skill was similar at both tidal
747 and subtidal time scales, and in three regions (the estuary, plume, and shelf). Tidal
748 properties were best modeled within the estuary, while subtidal T and S were best in
749 surface (<20 m depth) plume waters. Plume water properties were reasonably well-
750 represented by the model. For the 2004 summer simulation comparisons in the upper 20
751 m at a mooring in 72 m of water off the Columbia River mouth (Fig. 2) the model was on
752 average 1˚C too cool, and too fresh by 1 psu (MacCready et al., 2009). The subtidal RMS
753 error was 1.1˚C for T and 1.2 for S, while the tidal RMS error was 0.8˚C for T and 1.1 for
754 S (Liu et al., 2009b).

755 Of greater relevance for the scientific goals of the project, the ROMS model has
756 almost no mean bias in the near surface *stratification*, based on the difference between 1

757 m and 5 m T and S records (MacCready et al., 2009). Extensive model experimentation
758 demonstrated the crucial importance of open boundary conditions provided by NCOM
759 and correct bathymetry, such as estuary depth. The NCOM fields on the shelf appeared to
760 have a somewhat deeper thermocline and stronger southward flow than observed (Liu et
761 al., 2009b). These biases were less apparent in ROMS in the plume, presumably because
762 of the strong wind and river forcing. While statistical comparisons in the plume are
763 promising, some details of the plume structure are still incorrect. As one example, model
764 surface floats released near the Columbia River mouth on ebb tide did not penetrate as far
765 seaward as field drifters deployed during RISE observational campaigns (McCabe et al.,
766 2008). Select numerical experiments also illustrated that float-tracked surface plume
767 water may become too salty (mean salinity excess of ~3–4 psu). Other investigators have
768 found similar results in recent estuarine applications (e.g., Warner et al., 2005; Li et al.,
769 2005). The tidal plume is characterized by extremely high shear and stratification and
770 remains one of the most difficult-to-model physical environments in the coastal zone. To
771 this point, a hydrostatic model like ROMS necessarily omits details of the plume front
772 and the nonlinear internal waves it generates. Because of this we cannot simulate a
773 potentially large source of observed plume mixing.

774 The CORIE/SATURN modeling system is built with the philosophy of redundancy in
775 model, grids/domains, and modeling parameterizations. For any given period, daily
776 forecasts and multi-year simulation databases are conducted for at least two domains
777 (river-to-ocean and either estuary-only or estuary/near-plume), with river-to-ocean
778 simulations conducted with two models (SELFE and ELCIRC); only SELFE is used for
779 the estuary-only and estuary/near-plume domains. Simulations often explore multiple

780 parameterizations and the option exists to use model-independent data assimilation
781 strategies (Frolov et al., 2009a) for either improved process understanding (Frolov et al.,
782 200b) or observational network optimization (Frolov et al., 2008). Skill assessment has
783 been conducted for simulations based on both ELCIRC (Baptista et al., 2005; Burla et al.,
784 2009) and SELFE (Zhang and Baptista, 2008; Zhang et al., 2009; Burla et al., 2009), and
785 quantitative skill assessment metrics have recently become a part of routine processing of
786 all forecasts and simulation databases in the CORIE/SATURN modeling system
787 (http://www.stccmop.org). Quantitative skill metrics are based on comparisons with both
788 routine CORIE/SATURN observations and observations of opportunity (such as RISE
789 moorings and cruises). Highest skill is typically achieved with SELFE rather than with
790 ELCIRC, and (although often marginally) with hindcasts versus forecasts; during a
791 typical cruise, forecast skill was high enough to direct vessels within 2 km of a predicted
792 concentration more than 55% of the time (Zhang et al., 2009).
793 Typical SELFE/ELCIRC grid resolution is ~150 m in the estuary, 250 m–1 km in the
794 near-plume, and 3 km–20 km in the far plume. Skill typically decreases from the estuary
795 to the plume to the shelf outside the near-field plume, reflecting at least in part the
796 different resolution in each of these regions. For the plume, ELCIRC simulations have
797 shown a tendency for excess freshness (e.g., as a relatively extreme example, for 2004 the
798 ELCIRC model bias for salinity at a shelf mooring near the river mouth was -2.9 psu,
799 versus just -0.2 for SELFE; see Burla et al., 2009). SELFE was thus the preferred
800 CORIE/SATURN model for both near real-time forecasts in support of oceanographic
801 cruises (Zhang et al., 2009) and the calculation of multi-year time-series plume
802 characteristics such as volume, area, thickness and centroid location (Burla et al., 2009).

803 Although a systematic comparison between the ROMS and SELFE model
804 implementations for the Columbia plume has not been performed to date, examples of
805 their salinity and velocity fields are compared in Figure 10 for a) a period when the
806 plume tends northward and b) a period when the plume tends to the southwest. The
807 model runs were selected for dates when CTD transects were available. In addition,
808 satellite imagery (Fig. 1) is available within one day of the second model runs. The side-
809 by-side comparison highlights some qualitative differences between the models. The
810 most dramatic difference is that SELFE salinity structure has much less structure than
811 that of ROMS; this may be due to lower order numerics and interpolations associated
812 with the semi-Lagrangian time stepping in SELFE. The ROMS plumes in the examples
813 are generally fresher than the SELFE plumes in the plume far field (e.g., the fresh plume
814 tail south of about 46^{o}N in the upper panels). The stronger stratification of the ROMS
815 vertical salinity structure is more consistent with the observations available for these
816 snapshots for both north and southwest plumes. ROMS has much more upwelling at the
817 coast than SELFE—however the deep salinity in ROMS appears consistent with the
818 observations, and more consistent with the observations than the SELFE results. This
819 result may reflect differences in boundary forcing: the smaller domain NRL model used
820 in the ROMS formulation is expected to be more accurate than the larger domain Global
821 NRL model used for SELFE. With respect to the structure of the southwest-tending
822 plume, the ROMS plume appears less elongated than the SELFE plume. The blocky
823 shape (for this event at least) of the ROMS plume is consistent with satellite-derived
824 turbidity (see imagery in Figure 1 for one day after the model output). SELFE performs
825 slightly better than ROM in capturing the plume's east-west location on the shelf.

826 However, neither model does very well predicting cross shelf location in these two
827 snapshots: the northward modeled plumes have not spread offshore sufficiently compared
828 to both in situ data and the satellite figure; and the southwest tending plumes have spread
829 too far offshore in both models according to the in situ data.
830
831 c) *How well can we model plume biological influences?*
832 A four-box ("NPZD") ecosystem model was designed for the Columbia plume region,
833 parameterized and validated using an array of RISE observations: nutrients, chlorophyll,
834 microzooplankton biomass, phytoplankton community growth and grazing rates, and
835 process studies examining the phytoplankton response to light and nutrients (Banas et al.,
836 2009b; Lessard and Frame, 2008; Lessard et al., in prep.; Kudela and Peterson, 2009).
837 The diversity of these observations was key to the modeling effort, a rare opportunity to
838 take an empirical approach to the crucial problem of choosing free parameter values
839 (Friedrichs et al., 2007). Banas et al. (2009b) show that thus parameterized, even a very
840 simple model can pass unusually comprehensive (if not unusually precise) validation
841 tests: to our knowledge this is the first time that an ecosystem model of this type has been
842 compared with extensive simultaneous measurements of phytoplankton and zooplankton
843 biomass and community growth and grazing rates. The model correctly reproduces
844 plume-axis profiles of these quantities (Banas et al., 2009b, Fig. 8). Phytoplankton are at
845 moderate levels in the Columbia estuary and peak (in biomass and growth rate) in the
846 near-to-mid-field plume, while microzooplankton are low in the estuary and gradually
847 increase until a quasi-equilibrium between growth and grazing is reached in the far-field
848 plume (beyond ~40 km from the mouth). The model likewise reproduces the relationship

849 between the depletion of nutrients and increase in microzooplankton grazing pressure as
850 upwelled water parcels move offshore.
851 The significance of this model's accurate reproduction of not just stocks (nutrients
852 and biomass) but rates (primary production and microzooplankton grazing) is that the
853 rates are the real expression of the biological mechanisms and ecosystem dynamics at
854 work in the model. Without a validation of rates and fluxes (as is common, for lack of
855 data), one cannot be sure that stocks are being predicted for the right reasons; with such a
856 validation, we can have confidence in not just the model's mechanistic interpretation but
857 also in hypothetical cases. Banas et al. (2009b) also examined a case in which the
858 Columbia River was turned off in order to isolate plume effects on the coastal ecosystem.
859 Two effects of the plume on mean seasonal patterns were found, consistent with
860 observations, as mentioned above (Sec. 5.1): in the cross-shelf direction, a seaward shift
861 in primary production, and in the along-shelf direction, increased retention, which caused
862 a shift toward older communities and increased grazing.
863
864 5.3 Mixing Processes, Rates and Effects
865
866 a) *Where does mixing of river, plume and oceanic waters occur?*
867 Based on analyses of water mass properties (Bruland et al., 2008), turbulence
868 observations (Nash et al., 2009), and the modeled turbulent buoyancy flux (a proxy for
869 mixing of salt and fresh water) of MacCready et al. (2009), about half of the
870 transformation of fresh to oceanic salinity occurs in the estuary and lift-off or source
871 zone, and half over the shelf. However, the exact partitioning varies significantly with

872 differing wind, tide, and river flow conditions, but generally scales with Ri_E, the estuary
873 Richardson number (Fischer, 1972). Thus, when coastal waters are rich in nutrients, tidal
874 mixing in the plume, estuary and source zone represents a primary mechanism for
875 bringing high-nitrate, high-iron water into the plume. As a result, sufficient nitrate and
876 iron concentrations are established for maximum phytoplankton growth by the time river
877 water reaches the river mouth (Bruland et al., 2008). MacCready et al. (2009) indicate
878 that wind-driven mixing can account for most of the mixing on the shelf during periods
879 of neap tide and strong winds. Whether or not this mechanical forcing is biologically
880 relevant depends on the setting. During upwelling-favorable conditions, the southwest-
881 tending plume generally overlies, and is surrounded by, nutrient depleted surface waters.
882 In this case intermediate and far-field mixing is unlikely to provide further nutrient input
883 to the plume biomass. On the other hand, northward tending plumes frequently overlie
884 waters with high nitrate, so that wind-driven mixing could aid in fueling production.
885
886 b) *What processes determine the plume structure and composition?*
887 The tidal plume's initial composition (T, S, N) and vertical structure (thickness and
888 stratification) are largely set by turbulent processes in the estuary (Cudaback and Jay,
889 2000; Nash et al., 2009). Both observations (Nash et al., 2009) and model energy
890 analyses (MacCready et al., 2009) find turbulent dissipation within the estuary to be
891 primarily driven by the tidal bottom boundary stresses, with only secondary influences
892 from the shear associated with freshwater river flow. As a result, the near-field plume
893 salinity (and other properties such as amount of oceanic nitrate entrained, for example)
894 depends to first order on the balance between freshwater flux (i.e., riverflow Q_f), and

895 turbulent mixing, which scales with the cube of tidal velocity. The process is
896 conveniently described by the estuary Richardson number, which represents a
897 nondimensional ratio of Q_f to u^3. Since the estuary residence time is O(1–5 d), the
898 composition of the tidal plume varies with the neap-spring cycle and river flow
899 fluctuations.

900 As a result of this balance, Nash et al. (2009) show that periods of high riverflow
901 and/or weak tides produce relatively thin and highly-stratified plumes that detach from
902 the bottom. In contrast, during spring tides and/or weak river flow, plume stratification is
903 reduced, producing a deep river plume that remains in contact with the bottom for up to 5
904 km beyond the estuary mouth, suspending sediments (Spahn et al., 2009) and blocking
905 coastal flows. Once detached from the bottom, this stratification and thickness control the
906 propagation speed of the tidal plume front as it moves offshore as a buoyant gravity
907 current, its timing and ultimate extent determined by the strength of each ebb pulse
908 (Kilcher et al., 2009; Jay et al., 2009b). Its three dimensional structure is further modified
909 though coastal currents, which can deflect the plume front, alter its speed, and/or sharpen
910 horizontal gradients; and wind, which causes additional and chronic mixing in the aging
911 plume.

912 The evolution of tidal plume mixing was also explored with drifter data and
913 numerical simulations (McCabe et al., 2008, 2009). Surface drifters were deployed near
914 the mouth of the Columbia River on a few select ebb tides to track emerging plume
915 water. Conservation equations applied to adjacent drifters determined entrainment rates
916 following plume water as it advected and spread across the shelf. A significant finding is
917 that entrainment continued well beyond lift-off in the "tidal plume interior" as it spreads

laterally, suggesting that the spreading process helps maintain vertical mixing as the plume evolved at sea (McCabe et al., 2008). This observational study further illustrates how differences in plume deceleration, spreading, and thinning lead to entrainment, and qualitatively agrees with ROMS simulations showing significant interior stress and mixing throughout much of the spreading tidal plume (McCabe et al., 2009).

A theoretical model of the initial, supercritical (with respect to the internal Froude number, Fr) expansion of the Columbia tidal plume also shows that the depth of the tidal plume is controlled by a balance between thinning due to plume expansion and thickening due to entrainment (Jay et al., 2009b), echoing the observational analysis of McCabe et al. (2008). Based on the Jay et al. (2009b) model, the ratio of mass diffusivity to momentum diffusivity plays a significant role in plume properties, and both the barotropic and baroclinic pressure gradients contribute significantly to the plume momentum balance. Details of tidal plume dynamical balances and how they relate to lateral plume spreading are illustrated with realistic numerical simulations by McCabe et al. (2009). Those authors show that spreading largely results from a competition between the Coriolis force and flow-normal pressure gradient, and that plume interior stress is a primary factor acting to slow the plume.

During the ebb that forms each tidal plume, baroclinic shear sustains $R_i <= 0.25$ within the entire low-salinity surface layer, producing intense turbulence dissipation that scales with the strength of each pulse (Fig. 11; see also Nash et al., 2009); strong ebbs are ~10 times more dissipative than weak ones. In the stratified shear flow inshore of the plume front, turbulence dissipation rates are intense, decaying from $\sim 10^{-3}$ W kg^{-1} near the river mouth to $\sim 10^{-6}$–10^{-5} W kg^{-1} some 20 km offshore (Kilcher et al., 2009). Drifter data

941 (McCabe et al., 2008) also confirm that turbulent entrainment continues well after plume
942 liftoff and until the plume becomes geostrophically adjusted, at which point turbulence
943 approaches typical coastal levels. Within fronts, dissipation rates can be significantly
944 higher (Fig. 11; see also Orton and Jay, 2005; Kilcher et al., 2009; Jay et al., 2009a).
945
946 c) *How do nonlinear internal waves (NLIWs) affect the mixing at the Columbia*
947 *River plume frontal region?*
948 NLIWs may be generated when the plume front decelerates beneath the wave speed
949 for wave propagation (Nash and Moum, 2005). Jay et al. (2009a) showed that NLIW
950 were most commonly generated on the west and northwest sides of the tidal plume under
951 upwelling-favorable or weak wind conditions. They are much less commonly generated
952 during downwelling conditions. Moreover, the front first becomes subcritical (allowing
953 NLIW release) on its south side and southwest sides, regardless of wind direction. This
954 asymmetry is the result of transfer of vorticity to the plume by the underlying tidal flow.
955 Pan and Jay (2009) found that the ambient velocity shear alters the structure of the NLIW
956 by displacing the maximum of the NLIW vertical structure function as much as 5 m
957 below the density interface. This greatly affects NLIW-induced turbulent mixing at the
958 frontal region, because the displaced maximum internal wave shear is at a depth with
959 reduced stability, N^2. An analysis based on observations and internal wave theory
960 suggests that the vertical velocity shear is intensified primarily by the interaction between
961 sheared ambient velocity and the NLIW vertical structure at depths where the combined
962 NLIW and ambient shears result in $Ri_g<0.25$. Typically, neither mechanism acting alone
963 would drive mixing.

964

965 d) *How, where and when are plankton entrained into the plume*?

966 Based on the physical and chemical observations, it is clear that most of the turbulent
967 mixing in the plume occurs at the estuary bar and at the tidal plume front, over very short
968 timescales. There was no evidence for distinct plume plankton communities (Frame and
969 Lessard, 2009), and no evidence for distinct physiological responses in the plume versus
970 outside the plume (Kudela and Peterson, 2009). This is consistent with the plume
971 entraining and mixing plankton from the near-field coastal waters; while the plume has
972 strikingly different physical and chemical properties, it acts more as biological capacitor
973 (capturing nearshore coastal waters and sometimes adding nutrients), rather than serving
974 as a distinct source or sink for plankton.

975

976 e) *Does the regional plume have multiple physical, chemical or biological regions*
977 *or layers that can be distinguished?*

978 The water properties of the Columbia plume, which depend on the properties of both
979 river and ocean end members as well as the degree of mixing are extremely time-variable
980 as described above. Thus, it is difficult to ascribe specific values of properties to the
981 different plume regions, such as the source region (from the estuary mouth to about 5 km
982 upstream of the mouth), the tidal plume (the pulse of mixed river and shelf water
983 discharged onto the shelf during a single ebb tide; e.g., Fig. 11), or the aging plume
984 waters (sometimes referred to as the "far-field" plume). Nevertheless, property gradients
985 are usually sufficiently large that the tidal plume can be readily distinguished from aging
986 plume waters or deep water that has recently upwelled. The tidal plume overlays pre-

existing or aging plume waters, producing visible layers of salinity, temperature, density and nutrients (Horner-Devine et al., 2009). Although the estuarine source waters contain freshwater plankton species, because these rapidly die out on encountering oceanic waters, and are replaced by shelf species entrained during mixing, phytoplankton layers are less distinguishable. Significant differences in species composition and diatom composition between plume and oceanic waters have been documented during some plume events (Lessard and Frame, 2009).

Aguilar-Islas and Bruland (2006) demonstrated how elevated silicic acid and dissolved manganese could be used as chemical tracers of the far-field plume. Brown and Bruland (in press) showed how elevated dissolved and particulate aluminum in the Columbia River plume could be followed hundreds of km from the river mouth. The nitrate and much of the dissolved iron is rapidly assimilated by the phytoplankton, but the large excess of these other chemicals can serve to distinguish the plume. The dissolved manganese in the Columbia River estuary varies dramatically as a function of spring or neap tides (Aguilar-Islas and Bruland, 2006; Bruland et al., 2008). This can be used to distinguish aged plumes that formed under spring tide conditions from plumes that formed under neap tide conditions.

6. Conclusions

RISE studies have resulted in the development of a new working model of plume processes (Fig. 12). The cartoon illustrating this model shows plume processes in plan

1010 view as well as along sections emanating from the river mouth and downstream of the
1011 mouth. River and tidal waters (1-12 hr) are differentiated from aging (1-10 d and
1012 upwelling (1-10 d) waters. The cartoon reflects the modern picture of the Columbia
1013 plume: a plume with two branches, rather than simply a single southwest plume as
1014 depicted in the historic literature (Hickey et al., 2005; Liu et al., 2008). The northward
1015 branch of the Columbia plume in spring can, on occasion, transit the entire Washington
1016 shelf, wrap around the eddy offshore of the Strait of Juan de Fuca and return south to join
1017 newly emerging plume waters some 10–20 d later (Hickey et al., 2009).

1018 With respect to the three original RISE hypotheses given in the Introduction, 1)
1019 primary production has been shown to be higher in the newly emerging plume waters
1020 than on shelves outside the plume, and plume turbidity does not appear to inhibit growth
1021 (Fig. 12, panel a). 2) Model studies demonstrate that cross-shelf export is enhanced by
1022 about 20% by the presence of the river plume (panel c). Last, it has been shown that the
1023 area both north and south of the river mouth appear to be iron and silicate replete due to
1024 the presence of the Columbia plume (Bruland et al., 2008); in particular, iron limitation
1025 on phytoplankton growth is unlikely and diatoms are almost always dominant (Kudela et
1026 al., 2006; Frame and Lessard, 2009). This result fundamentally differentiates the northern
1027 CCS from coastal waters in the more southern parts of the CCS. No north-south rate
1028 differences due to silicate or iron supply were documented.

1029 A number of other important improvements in understanding how freshwater mixes
1030 into the coastal ocean and how the resulting plume affects the local ecosystem have
1031 emerged from RISE. For example, in situ measurements and model studies demonstrated
1032 where mixing occurs and the magnitude of mixing rates, which decrease with distance

from the river mouth (Nash et al., 2009; MacCready et al., 2009). Nonlinear internal waves, generated on the west/northwest side of the plume under upwelling-favorable or weak wind conditions (Fig. 12, panel c), also affect mixing of plume water (Jay et al., 2009a). About half the mixing occurs inside the estuary and near the mouth, with the remainder occurring primarily as a result of wind mixing as the plume ages. Nitrate (during upwelling periods) and plankton are both entrained into the plume in the estuary and near mouth mixing; the plume in general does not contain unique plankton assemblages. The river itself can contribute nitrate to the plume with generally low concentrations in summer, and higher concentrations in spring (Fig. 12, panel a). Although these amounts are small when seasonally integrated in comparison to that supplied by regional upwelling (Hickey and Banas, 2008), they are sufficient to sustain the local ecosystem during periods of extended downwelling or delayed seasonal upwelling (Bruland et al., 2008). Model results show that tidal dynamics on the shelf near the estuary enhances nitrate supply from the ocean during upwelling events (Hickey and Banas, 2008). Although nitrate supply in the plume is usually moderate to high, phytoplankton become nitrate limited as plume waters age (Fig. 12, panel b). With respect to zooplankton, RISE data confirm that macrozooplankton aggregate near Columbia plume fronts (Peterson and Peterson, 2009). Microzooplankton grazing is lowest in the plume, and higher over shelves south of the river mouth than north of it (Frame and Lessard, 2009).

The fundamental RISE question was:

To what extent is the Columbia River plume the cause of the north-south gradient in chlorophyll concentration in the Pacific Northwest?

RISE confirmed that chlorophyll concentrations are generally higher north of the Columbia mouth than south of it, over the ~150 km between measurement transects. However, contrary to expectations, growth rates and physiological status of the phytoplankton were similar to the north and south, rather than increasing to the north in conjunction with chlorophyll. One of the most important effects of the Columbia plume on alongcoast gradients is that it acts as a north-south barrier to biomass transport (Fig. 12, panel c), deflecting biomass seaward of the Oregon shelf; it channels biomass accumulated on the Washington shelf, much of which originates on the shelf well north of the plume, offshore so that it misses the Oregon shelf. The Oregon shelf essentially has to reset its own phytoplankton community from local upwelling without the addition of an upstream source.

The data clearly demonstrate that upwelling is more frequent and of longer duration off the Oregon coast than off the Washington coast, where wind stress is weaker, and also where plume waters often "cap" upwelling. Nevertheless, the nitrate supply in shelf bottom waters was always greater to the north, and is likely due to some combination of remote wind forcing, submarine canyon upwelling enhancement, and the enhanced upwelling near the Strait of Juan de Fuca and its offshore eddy (Hickey and Banas, 2008; MacFadyen et al., 2008). In combination with the higher grazing pressure off Oregon documented in RISE (Frame and Lessard, 2009), these data suggest that the northward chlorophyll increase is due to a combination of top-down (grazing) and bottom-up

(nitrate) effects, with some partial blocking effect by the plume which makes northern Oregon a "shadow zone". Although the spatial pattern of grazing likely reflects the influence of the plume (Banas et al., 2008), enhanced nitrate supply to the northern Washington shelf is not related to the plume.

Thus the Columbia plume does indeed appear to be instrumental in making the southern Washington coast such a rich ecosystem, both through increased supply of nutrients and increased retention of nutrients and biomass; but the northern source of nutrients and biomass appears to play just as significant a role. Accordingly, future studies of these processes must expand in scale, to encompass the interactions between freshwater inputs and retention features over hundreds of kilometers of coastline.

Acknowledgements

This summary was supported by grant #OCE-0239089 to B. Hickey, P. MacCready and E. Lessard; #OCE-0238347 to K. Bruland and R. Kudela; #OCE-0238021to E. Dever; # OCE-0238727 to J. Nash and J. Moum; #OCE-0237710 to M. Kosro; # OCE-0622278 and #OCE-0239072 to D. Jay and A. Baptista; and #OCE-0239107 to W. Peterson from the National Science Foundation (NSF) as part of the Coastal Ocean Processes RISE Program. The CORIE/SATURN observation and prediction system is scientific infrastructure of the NSF Science and Technology Center for Coastal Margin Observation and Prediction and is also partially supported by regional stakeholders, including the National Oceanic and Atmospheric Administration and the Bonneville

Power Administration. The authors would like to thank the captains and crews of the R/V Wecoma and Pt. Sur for their outstanding support of this research. RISE would not have been successful without the combined efforts of numerous staff and students from each of the research teams; in particular, Nancy Kachel, Susan Geier, Mike Foy, Megan Bernhardt, David Darr, Sherry Palacios, Misty Blakely, Bettina Sohst, Geoffrey Smith, and Keith Leffler. This is contribution #xx of the RISE program. The statements, findings, conclusions, and recommendations are those of the authors and do not necessarily reflect the views of NSF.

References

Aguilar-Islas, A. M., and K. W. Bruland (2006), Dissolved manganese and silicic acid in the Columbia River plume: A major source to the California current and coastal waters off Washington and Oregon, *Marine Chemistry*, *101*(3–4), *233–247*.

Bakun, A. (1973), Coastal upwelling indices, west coast of North America, 1946–71. NOAA Techn. Rept. NMFS SSRF-671, 103 pp., US Dept. of Commerce, Washington DC.

Banas, N. S., P. MacCready, and B. M. Hickey (2009a), The Columbia River plume as cross-shelf exporter and along-coast barrier, *Cont. Shelf Res.*, *29*(1), 292–301, doi:10.1016/j.csr.2008.03.011.

Banas, N. S., E. J. Lessard, R. M. Kudela, P. MacCready, T. D. Peterson, B. M. Hickey, and E. Frame (2009b), Planktonic growth and grazing in the Columbia River plume region: A biophysical model study, *J. Geophys. Res*. (this volume).

Baptista, A. M. (2006), CORIE: the first decade of a coastal-margin collaborative observatory, Oceans 2006, MTS/ IEEE, Boston, MA.

Baptista, A. M., Y. Zhang, A. Chawla, M. Zulauf, C. Seaton, E. P. Myers, J. Kindle, M. Wilkin, M. Burla, and P. J. Turner (2005), A cross-scale model for 3D baroclinic circulation in estuary-plume-shelf systems: II. Application to the Columbia River, *Cont. Shelf Res.*, *25*, 935–972.

Barnes, C. A., A. C. Duxbury, and B. A. Morse (1972), Circulation and selected properties of the Columbia River effluent at sea, in *The Columbia River Estuary and*

Adjacent Ocean Waters, edited by A. T. Pruter and D. L. Alverson, pp. 41–80, Univ. Washington Press, Seattle, WA.

Barron, C. N., A. B. Kara, P. J. Martin, R. C. Rhodes, and L. F. Smedstad (2006), Formulation, implementation and examination of vertical coordinate choices in the global Navy Coastal Ocean Model (NCOM), *Ocean Model.*, *11*(3–4), 347–375.

Battisti, D., and B. M. Hickey (1984), Application of remote wind forced coastal trapped wave theory to the Oregon and Washington coasts, *J. Phys. Oceanogr.*, *14*, 887–903.

Bi, H., R. E. Ruppel, W. T. Peterson (2007), Modeling the salmon pelagic habitat off the Pacific Northwest (USA) coast using logistic regression. *Mar. Ecol. Prog. Ser.*, *336, 249–265.*

Boicourt, W. C., W. J. Wiseman, Jr., A. Valle-Levinson, and L. P. Atkinson (1998), Continental shelf of the southeastern United States and the Gulf of Mexico: In the shadow of the Western Boundary Current, in *The Sea, Vol. 11*, edited by A. R. Robinson and K. H. Brink, pp. 135–182, John Wiley & Sons, Inc., New York.

Bottom, D. L., C. A. Simenstad, J. Burke, A. M. Baptista, D. A. Jay, K. K. Jones, E. Casillas, and M. H. Schiewe (2005), Salmon at river's end: The role of the estuary in the decline and recovery of Columbia River salmon. NOAA Tech. Memo., NMFS-NWFSC-68, 246 pp., U.S. Dept. of Commerce.

Brown, M. T., and K. W. Bruland. Dissolved and particulate aluminum in the Columbia River and coastal waters of Oregon and Washington: behavior in near-field and far-field plumes. *Estuarine, Coastal and Shelf Science*, In Press.

1151 Bruland, K. W., E. L. Rue, and G. J. Smith (2001), Iron and macronutrients in California
1152 coastal upwelling regimes: Implications for diatom blooms, *Limnol. Oceanogr.*, *46*,
1153 1661–1674.

1154 Bruland, K. W., M. C. Lohan, A. M. Aguilar-Islas, G. J. Smith, B. Sohst, and A. Baptista
1155 (2008), Factors influencing the chemistry and formation of the Columbia River
1156 Plume: Nitrate, silicic acid, dissolved Fe and dissolved Mn, *J. Geophys. Res*. *113*,
1157 C00B02, doi:10.1029/2007JC004702.

1158 Burla, M., A. M. Baptista, Y. Zhang, and S. Frolov (2009), Seasonal and inter-annual
1159 variability of the Columbia River plume: A perspective enabled by multi-year
1160 simulation databases, *J. Geophys. Res.* (this volume).

1161 Chao, S.-Y., and W. C. Boicourt (1986), Onset of estuarine plumes, *J. Phys. Oceanogr.*,
1162 *16*, 2137–2149.

1163 Chase, Z., A. van Geen, P. M. Kosro, J. Marra, and P. A. Wheeler (2002), Iron, nutrient,
1164 and phytoplankton distributions in Oregon coastal waters, *J. Geophys. Res.*,
1165 *107*(C10), 3174, doi:10.1029/2001JC000987.

1166 Chase, Z., P. Strutton, and B. Hales (2007), Iron links river runoff and shelf width to
1167 phytoplankton biomass along the U.S. West Coast, *Geophys. Res. Lett.*, *34*, L04607,
1168 doi:10.1029/2006GL028069.

1169 Chawla, A., D. A. Jay, A. M. Baptista, M. Wilkin, and C. Seaton (2008), Seasonal
1170 variability and estuary-shelf interactions in circulation dynamics of a river-dominated
1171 estuary, *Estuaries Coasts*, *31*, 269–288, doi:10.1007/s12237-007-9022-7.

1172 Conomos, T. J., M. G. Gross, C. A. Barnes, and F. A. Richards (1972), River-ocean
1173 nutrient relations in summer, in *The Columbia River Estuary and Adjacent Ocean*
1174 *Waters*, edited by A. T. Pruter and D. L. Alverson, pp. 151–175, Univ. Washington
1175 Press, Seattle, WA.

1176 Cudaback, C. N., and D. A. Jay (2000), Tidal asymmetry in an estuarine pycnocline:
1177 Depth and thickness, *J. Geophys. Res.*, *105*, 26237–26252.

1178 Cudaback, C. N., and D. A. Jay (2001), Tidal asymmetry in an estuarine pycnocline 2.
1179 Transport, *J. Geophys. Res*., *106*(C2), 2639–2652.

1180 De Robertis, A., C. A. Morgan, R. A. Schabetsberger, R. W. Zabel, and 5 others (2005),
1181 Columbia River plume fronts, II: Distribution, abundance, and feeding ecology of
1182 juvenile salmon, *Mar. Ecol. Prog. Ser., 299*, 33–44.

1183 Dracup, J. A., and E. Kahya (1994), The relationships between U.S. streamflow and La
1184 Niña events, *Water Resour. Res.*, *30*, 2133–2141.

1185 Fain, A. M. V., D. A. Jay, D. J. Wilson, P. M. Orton, and A. M. Baptista (2001),
1186 Seasonal, monthly and tidal patterns of particulate matter dynamics in the Columbia
1187 River estuary, *Estuaries Coasts*, *24*, 770–786.

1188 Firme, G. F., E. L. Rue, D. A. Weeks, K. W. Bruland, and D. A. Hutchins (2003), Spatial
1189 and temporal variability in phytoplankton iron limitation along the California coast
1190 and consequences for Si, N and C biogeochemistry. *Global Biogeochem. Cycles*, *17*,
1191 1016.

1192 Fischer, H. B. (1972), Mass transport mechanisms in partially stratified estuaries, *J. Fluid*
1193 *Mech.*, *53*(4), 671–687.

1194 Fong, D., and W. R. Geyer (2002), The alongshore transport of fresh water in a surface-
1195 trapped river plume, *J. Phys. Oceanogr.*, *32*(3), 957–972.
1196
1197 Frame, E. R., and E. J. Lessard (2009), Does the Columbia River Plume influence
1198 phytoplankton community structure along the Washington and Oregon coasts?, *J.*
1199 *Geophys. Res.* (this volume).

1200 Friedrichs, M. A. M., J. A. Dusenberry, L. A. Anderson, R. A. Armstrong, F. Chai, J. R.
1201 Christian, S. C. Doney, J. Dunne, M. Fujii, R. Hood, D. J. McGillicuddy Jr., J. K.
1202 Moore, M. Schartau, Y. H. Spitz, and J. D. Wiggert (2007), Assessment of skill and
1203 portability in regional marine biogeochemical models: Role of multiple planktonic
1204 groups, *J. Geophys. Res.*, *112*, C08001, doi:10.1029/2006JC003852.

1205 Frolov, S., A. M. Baptista, and M. Wilkin (2008), Optimizing fixed observational assets
1206 in a coastal observatory, *Cont. Shelf. Res.*, *28*(19), 2644–2658,
1207 doi:10.1016/j.csr.200808.009.

1208 Frolov, S., A. M. Baptista, T. Leen, Z. Lu, and R. van der Merwe (2009a), Fast data
1209 assimilation using a nonlinear Kalman filter and a model surrogate: An application to
1210 the Columbia River estuary, *Dyn. Atmos. Oceans*,
1211 doi:10.1016/jdynatmoce.2008.10.004, in press.

1212 Frolov, S., A.M. Baptista, Y. Zhang, and C. Seaton (2009b), Estimation of ecologically
1213 significant circulation features of the Columbia River Estuary and Plume using a

reduced-dimension Kalman Filter, *Cont. Shelf Res*., *29*(2), 456–466, doi:10.1016/j.csr.2008.11.004.

Garcia-Berdeal, I., B. M. Hickey, and M. Kawase (2002), Influence of wind stress and ambient flow on a high discharge river plume, *J. Geophys. Res.*, *107*(C9), 3130, doi:10.1029/2001JC000932.

Garvine, R. W. (1982), A steady state model for buoyant surface plume hydrodynamics in coastal waters, *Tellus, 34*, 293–306.

Garvine, R. W. (1999), Penetration of buoyant coastal discharge onto the continental shelf: a numerical model experiment, *J. Phys. Oceanogr.*, *29*, 1892–1909.

Gershunov A., T. P. Barnett, and D. R. Cayan (1999), North Pacific interdecadal oscillation seen as factor in ENSO-related North American climate anomalies, *EOS*, *Trans. Am. Geophys. Union*, *80*(3), 25.

Giese, B. S., and D. A. Jay (1989), Modelling tidal energetics of the Columbia River estuary, *Estuar. Coast. Shelf Sci.*, *29*(6), 549–571.

Grimes, C. B., and M. J. Kingsford (1996), How do riverine plumes of different sizes influence fish larvae: Do they enhance recruitment?, *Mar. Freshwater Res.*, *47*, 191–208.

Hamilton, P. (1990), Modelling salinity and circulation for the Columbia River Estuary, *Prog. Oceanogr.*, *25*(1–4), 113–156.

Hickey, B. M. (1979), The California current system—Hypotheses and facts, *Prog. Oceanogr.*, *8*, 191–279.

1235 Hickey, B. M. (1989), Patterns and processes of shelf and slope circulation, in *Coastal*
1236 *Oceanography of Washington and Oregon*, edited by M. R. Landry and B. M.
1237 Hickey, pp. 41–115, Elsevier Science, Amsterdam, The Netherlands.

1238 Hickey, B. M. (1998), Coastal Oceanography of Western North America from the tip of
1239 Baja California to Vancouver Is., in *The Sea*, vol. 11, edited by K. H. Brink and A. R.
1240 Robinson, pp. 345–393, John Wiley and Sons, Inc., New York.

1241 Hickey, B. M., and N. Banas (2003), Oceanography of the Pacific Northwest coastal
1242 ocean and estuaries with application to coastal ecosystems, *Estuaries Coasts*, *26*(48),
1243 1010–1031.

1244 Hickey, B. M., and N. Banas (2008), Why is the northern California Current so
1245 Productive?, *Oceanogr. Soc*., *21*(4), 90–107.

1246 Hickey, B. M., L. J. Pietrafesa, D. A. Jay, and W. C. Boicourt (1998), The Columbia
1247 River plume study, Subtidal variability in the velocity and salinity fields, *J. Geophys.*
1248 *Res*., *103*, 10339–10368.

1249 Hickey, B., S. Geier, N. Kachel, and A. MacFadyen (2005), A bi-directional river plume: The
1250 Columbia in summer, *Cont. Shelf Res.*, *25*(14), 1631–1656.

1251 Hickey, B. M., A. MacFadyen, W. P. Cochlan, R. M. Kudela, K. W. Bruland, and C. R.
1252 Trick (2006), Evolution of biological, chemical and physical water properties in the
1253 Pacific Northwest in 2005: Remote or local wind forcing?, *Geophys. Res. Lett.*, *33*,
1254 L22S02, doi:10.1029/2006GL026782.

1255 Hickey, B., R. McCabe, S. Geier, E. Dever, and N. Kachel (2009), Three interacting

freshwater plumes in the Northern California Current System, *J. Geophys. Res.*, *114*, C00B03, doi:10.1029/2008JC004907.

Hooff, R. C., and W. T. Peterson (2006), Recent increases in copepod biodiversity as an indicator of changes in ocean and climate conditions in the northern California current ecosystem, *Limnol. Oceanogr.*, *51*, 2042–2051.

Horner-Devine, A. R. (2009), The bulge circulation in the Columbia River plume, *Cont. Shelf Res*., *29*(1), 234–251, doi:10.1016/j.csr.2007.12.012.

Horner-Devine, A., D. Fong, S. Monismith, and T. Maxworthy (2006), Laboratory experiments simulating a coastal river inflow, *J. Fluid Mech.*, *555*, 203–232, doi:10.1017/S0022112006008937.

Horner-Devine, A. R., D. A. Jay, P. M. Orton, and E. Spahn (2009), A conceptual model of the strongly tidal Columbia River plume, *J. Mar. Syst*., doi:10.1016/j.jmarsys.2008.11.025, in press.

Hughes, R. P., and M. Rattray (1980), Salt flux and mixing in the Columbia River Estuary, *Est. Coast. Mar. Sci.*, *10*, 479–494.

Hutchins, D. A., and K.W. Bruland (1998), Iron-limited diatom growth and Si:N uptake ratios in a coastal upwelling regime, *Nature*, *393*, 561–564.

Hutchins, D. A., G. R. DiTullio, Y. Zhang, and K. W. Bruland (1998), An iron limitation mosaic in the California upwelling regime, *Limnol. Oceanogr.*, *43*, 1037–1054.

Huyer, A., E. J. C. Sobey, and R. L. Smith (1979), The spring transition in currents over the Oregon continental shelf, *J. Geophys. Res.*, *84*(C11), 6995–7011.

1277 Jay, D. A., and J. D. Smith (1990a), Circulation, density distribution and neap-spring
1278 transitions in the Columbia River Estuary, *Prog. Oceanogr.*, *25*, 81–112.

1279 Jay, D. A., and J. D. Smith (1990b), Residual circulation in shallow estuaries: 1. Highly
1280 stratified, narrow estuaries, *J. Geophys. Res.*, *95*(1), 711–731.

1281 Jay, D. A., and J. D. Smith (1990c), Residual circulation in shallow estuaries. 2. Weakly
1282 stratified and partially mixed, narrow estuaries, *J. Geophys. Res., 95*(C1), 733–748.

1283 Jay, D. A., and J. D. Musiak (1996), Internal tidal asymmetry in channel flows: origins
1284 and consequences, in *Mixing in Estuaries and Coastal Seas, Coastal and Estuarine*
1285 *Studies*, vol 50, edited by C. Pattiaratchi, pp. 219–258, AGU, Washington, D. C.

1286 Jay, D. A., J. Pan, P. M. Orton, and A. Horner-Devine (2009a), Asymmetry of tidal
1287 plume fronts in an eastern boundary current regime, *J. Marine Syst.*, in press.

1288 Jay, D. A., E. D. Zaron, and J. Pan (2009b), Initial expansion of the Columbia River tidal
1289 plume, *J. Geophys. Res.* (this volume).

1290 Kay, D. J., and D. A. Jay (2003a), Interfacial mixing in a highly stratified estuary 1.
1291 Characteristics of mixing, *J. Geophys. Res*., *108*(C3), 3072,
1292 doi:10.1029/2002JC000252.

1293 Kay, D. J., and D. A. Jay (2003b), Interfacial mixing in a highly stratified estuary 2. A
1294 "method of constrained differences" approach for the determination of the momentum
1295 and mass balances and the energy of mixing, *J. Geophys. Res*., *108*(C3), 3073,
1296 doi:10.1029/2002JC000253.

1297 Kilcher, L. (2008), Turbulence in river plumes, *Oceanography*, *21*(4), 31.

1298 Kilcher, L., J. Nash, and J. Moum (2009), Evolution of the Columbia River tidal plume
1299 front, *J. Geophys. Res.* (In Prep.).

1300 Kosro, P. M. (2005), On the spatial structure of coastal circulation off Newport, Oregon,
1301 during spring and summer 2001, in a region of varying shelf width, *J. Geophys. Res.*,
1302 *110*(C10), doi:10.1029/2004JC002769.

1303 Kosro, P. M., W. T. Peterson, B. M. Hickey, R. K. Shearmann, and S. D. Pierce (2006),
1304 Physical versus biological spring transition, *Geophys. Res. Lett.*, *33*, L22S03,
1305 doi:10.1029/2006GL027072.

1306 Kudela, R., W. Cochlan, T. Peterson, and C. Trick (2006), Impacts on phytoplankton
1307 biomass and productivity in the Pacific Northwest during the warm ocean conditions
1308 of 2005, *Geophys. Res. Lett.*, *33*, L22S06, doi:10.1029/2006GL026772.

1309 Kudela, R. M., and T. D. Peterson (2009), Influence of a buoyant river plume on
1310 phytoplankton nutrient dynamics: What controls standing stocks and productivity?, *J.*
1311 *Geophys. Res*. (this volume).

1312 Landry, M. R., and B. M. Hickey (Eds.) (1989), *Coastal Oceanography of Washington*
1313 *and Oregon*, 607 pp., Elsevier Science, Amsterdam, The Netherlands.

1314 Landry, M. R., and C. J. Lorenzen (1989), Abundance, distribution, and grazing impact
1315 of zooplankton on the Washington shelf, in *Coastal Oceanography of Washington*
1316 *and Oregon*, edited by M. R. Landry and B. M. Hickey, pp. 175–202, Elsevier
1317 Science, Amsterdam, The Netherlands.

1318 Landry, M. R., J. R. Postel, W. K. Peterson, and J. Newman (1989), Broad-scale
1319 distributional patterns of hydrographic variables on the Washington/Oregon shelf, in
1320 *Coastal Oceanography of Washington and Oregon*, edited by M. R. Landry and B.
1321 M. Hickey, pp. 1–40, Elsevier Science, Amsterdam, The Netherlands.

1322 Legaard, K. R, and A. C. Thomas (2006), Spatial patterns in seasonal and interannual
1323 variability of chlorophyll and sea surface temperature in the California Current, *J.*
1324 *Geophys. Res.*, *111*, C06032, doi:10.1029/2005JC003282.

1325 Lessard, E. J., and E. R. Frame (2008), The influence of the Columbia River Plume on
1326 patterns of phytoplankton growth, grazing and chlorophyll on the Washington and
1327 Oregon coasts. 2008 Ocean Sciences Meeting, AGU/ASLO/TOS/ERF, Orlando, FL.

1328 Lessard, E. J., E. R. Frame, M. B. Olson, M. S. Foy, and M. Bernhardt. Patterns and
1329 control of phytoplankton growth, grazing and chlorophyll on the northeast Pacific
1330 coast. *Limnol. Oceanogr*. In Prep.

1331 Li, M., L. Zhong, and W. C. Boicourt (2005), Simulations of Chesapeake Bay estuary:
1332 sensitivity to turbulence mixing parameterizations and comparison with observations,
1333 *J. Geophys. Res.*, *110*, C12004, doi:10.1029/2004JC002585.

1334 Liu, Y., P. MacCready, and B. M. Hickey (2009a), Columbia River Plume patterns as
1335 revealed by a hindcast coastal ocean circulation model in summer 2004, *Geophys.*
1336 *Res. Lett.*, *36*, L02601, doi:10.1029/2008GL036.

1337 Lippiatt, S. M., M. T. Brown, M. C. Lohan, C. J. M. Berger, and K.W. Bruland (2009)
1338 Leachable particulate iron in the Columbia River, estuary and near-field plume.
1339 Estuarine, *Coastal and Shelf Science*, submitted.

1340 Liu, Y., P. MacCready, B. M. Hickey, E. P. Dever, P. M. Kosro, and N. S. Banas
1341 (2009b), Evaluation of a coastal ocean circulation model for the Columbia River
1342 Plume in summer 2004, *J. Geophys. Res.* (this volume).

1343 Lohan, M. C., and K. W. Bruland (2006), Importance of vertical mixing for additional
1344 sources or nitrate and iron to surfaces waters of the Columbia River Plume:
1345 Implications for biology, *Mar. Chem*. 98, 260-273.

1346 Lohan, M. C., and K. W. Bruland (2008), Elevated Fe(II) and total dissolved Fe in
1347 hypoxic shelf waters off the coast of Washington and Oregon: An enhanced source of
1348 iron to coastal upwelling regimes*, Environ. Sci. and Tech., 42(17)*, 6462-6468, doi:
1349 10.1021/es800144j.

1350 Lohrenz, S. E, G. L. Fahnenstiel, D. F. Millie, O. M. E. Schofield, T. Johengen, and T.
1351 Bergmann (2004), Spring phytoplankton photosynthesis, growth, and primary
1352 production and relationships to a recurrent sediment plume and river inputs in
1353 southeastern Lake Michigan, *J. Geophys. Res.*, *109*, C10S14,
1354 doi:10.1029/2004JC002383.

1355 MacCready, P., N. S. Banas, B. H. Hickey, E. P. Dever, and Y. Liu (2009), A model
1356 study of tide- and wind-induced mixing in the Columbia River Estuary and Plume,
1357 *Cont. Shelf Res.*, *29*(1), 278–291, doi:10.1016/j.csr.2008.03.015.

1358 MacFadyen, A., B. M. Hickey, and M. G. G. Foreman (2005), Transport of surface
1359 waters from the Juan de Fuca Eddy region to the Washington coast: Implications for
1360 HABs, *Cont. Shelf Res*., *25*, 2008–2021.

1361 MacFadyen, A., B. M. Hickey, and W. P. Cochlan (2008), Influences of the Juan de Fuca

1362 Eddy on circulation, nutrients, and phytoplankton production in the northern
1363 California Current System, *J. Geophys. Res*., *113*, C08008,
1364 doi:10.1029/2007JC004412.

1365 Mantua, N. J., S. R. Hare, Y. Zhang, J. M. Wallace, and R. C. Francis (1997), A Pacific
1366 interdecadal climate oscillation with impacts on salmon production, *Bull. Amer.*
1367 *Meteor. Soc.*, *78*, 1069–1079.

1368 Mass, C., and 21 co-authors (2003), Regional environmental prediction over the Pacific
1369 Northwest, *Bull. Amer. Meteor. Soc.*, *84*, 1353–1366.

1370 McCabe, R., B. Hickey, and P. MacCready (2008), Observational estimates of
1371 entrainment and vertical salt flux behind the frontal boundary of a spreading river
1372 plume, *J. Geophys. Res.*, *113*, C08027, doi:10.1029/2007JC004361.

1373 McCabe, R. M., P. MacCready, and B. M. Hickey (2009), Ebb tide dynamics and
1374 spreading of a large river plume, *J. Phys. Oceanogr.*, submitted.

1375 Morgan, C. A., A. De Robertis, and R. W. Zabel (2005), Columbia River plume fronts, I:
1376 Hydrography, zooplankton distribution, and community composition, *Mar. Ecol.*
1377 *Prog. Ser.*, *299*, 19–31.

1378 Nash, J. D., and J. N. Moum (2005), River plumes as a source of large-amplitude internal
1379 waves in the coastal ocean, *Nature*, *437*, 400–403, doi:10.1038/nature03936.

1380 Nash, J. D., L. Kilcher, and J. N. Moum (2009), Turbulent mixing in the Columbia River
1381 Estuary: Structure and consequences for plume composition, *J. Geophys. Res.* (this
1382 volume).

1383 Nittrouer, C. A. (1978), The process of detrital sediment accumulation in a continental
1384 shelf environment: an examination of the Washington shelf, Ph.D. dissertation, 243
1385 pp., Univ. Washington, Seattle, WA.

1386 Orton, P. M., and D. A. Jay (2005), Observations at the tidal plume front of a high
1387 volume river outflow, *Geophys. Res. Lett.*, *32*, L11605, doi:10.102/2005GL022372.

1388 Pan, J., and D. A. Jay (2009), Effects of ambient velocity shear on internal solitons and
1389 associated mixing at the Columbia River front, *J. Geophys. Res.* (this volume).

1390 Pearcy, W. G. (1992), *Books in Recruitment Fishery Oceanography: Ocean Ecology of*
1391 *North Pacific Salmonids*, 179 pp., Univ. Washington Press, Seattle, WA.

1392 Peterson, J. O., and W. T. Peterson (2008), Influence of the Columbia River plume
1393 (USA) on the vertical and horizontal distribution of mesozooplankton over the
1394 Washington and Oregon shelf, *ICES J. of Mar. Sci.*, *65*, 477–483.

1395 Peterson, J. O., and W. T. Peterson (2009), The influence of the Columbia River plume
1396 on cross-shelf transport of zooplankton, *J. Geophys. Res.* (this volume).

1397 Pierce, D. P., J. A. Barth, R. E. Thomas, and G. W. Fleischer (2006), Anomalously warm
1398 July 2005 in the northern California Current: Historical context and the significance
1399 of cumulative wind stress, *Geophys. Res. Lett.*, *33*, L22S04,
1400 doi:10.1029/2006GL027149.

1401 Pruter, A. T., and D. L. Alverson (1972), *The Columbia River Estuary and Adjacent*
1402 *Coastal Waters*, 868 pp., Univ. Washington Press, Seattle, WA.

1403 Roegner, C., B. M. Hickey, J. Newton, A. Shanks, and D. Armstrong (2002), Estuarine-
1404 nearshore links during a coastal upwelling cycle: Plume and bloom intrusions into
1405 Willapa Bay, Washington, *Limnol. Oceanogr*., *47*(4), 1033–1042.

1406 Shaw, T. C., L. R. Feinberg, and W. T. Peterson (2009), Interannual variations in vital
1407 rates of copepods and euphausiids during the RISE study 2004–2006, *J. Geophys.*
1408 *Res.* (this volume).

1409 Shulman, I., J. C. Kindle, S. deRada, S. C. Anderson, B. Penta, and P. J. Martin (2004),
1410 Development of a hierarchy of nested models to study the California Current System,
1411 in *Estuarine and Coastal Modeling*, edited by M. L. Spaulding, pp. 74–88,
1412 Proceedings of 8th International Conference on Estuarine and Coastal Modeling,
1413 Monterey, CA, USA.

1414 Simenstad, C. A., L. Small, C. D. McIntire, D. A. Jay, and C. R. Sherwood (1990a),
1415 Columbia River estuary studies: An introduction to the estuary, a brief history,
1416 and prior studies, *Prog. Oceanogr*., *25,* 1–14.

1417 Simenstad, C. A., C. D. McIntire, and L. F. Small (1990b), Consumption processes and
1418 food web structure in the Columbia River estuary, *Prog. Oceanogr*., *25,* 271–298.

1419 Small, L. F., C. D. Mcintire, K. B. Macdonald, J. R. Laralara, B. E. Frey, M. C.
1420 Amspoker, and T. Winfield (1990), Primary production, plant and detrital biomass,
1421 and particle transport in the Columbia River Estuary, *Prog. Oceanogr.*, *25*, 175–210.

1422 Spahn, E. Y., A. R. Horner-Devine, D. A. Jay, J. Nash, and L. Kilcher (2009), Particle re-
1423 suspension in the Columbia River plume near-field, *J. Geophys. Res.* (this volume).

1424 Strub, P. T., J. S. Allen, A. Huyer, and R. L. Smith (1987), Large-scale structure of the spring
1425 transition in the coastal ocean off western North America, *J. Geophys. Res.*, *92*(C2), 1527–
1426 1544.

1427 Strub, P. T., C. James, A. C. Thomas, and M. R. Abbott (1990), Seasonal and non-seasonal
1428 variability of satellite-derived surface pigment concentration in the California Current. *J.*
1429 *Geophys. Res.*, *95*, 11501-11530.

1430 Sullivan, B. E., F. G. Prahl, L. F. Small, and P. A. Covert (2001), Seasonality of
1431 phytoplankton production in the Columbia River: A natural or anthropogenic
1432 pattern?, *Geochim. Cosmochim. Acta*, *65*, 1125–1139.

1433 Swartzman, G. and B. Hickey (2003), Evidence for a regime shift after the 1997-1998 El
1434 Niño, based on 1995, 1998 and 2001 acoustic surveys in the Pacific Eastern
1435 Boundary Current, *Estuaries, 26* (4B): 1032-1043.

1436 Thomas, A. C., M. E. Carr, and P. T. Strub (2001), Chlorophyll variability in eastern
1437 boundary Currents, *Geophys. Res. Lett.*, *28*, 3421–3424.

1438 Thomas, A. C., and R. Weatherbee (2006), Satellite-measured temporal variability of the
1439 Columbia River plume, *Rem. Sensing Env.*, *100*, 167–178.

1440 Venegas, R., P. Strub, E. Beier, R. Letelier, A. Thomas, T. Cowles, C. James, L. Soto-
1441 Mardones, and C. Cabrera (2008), Satellite-derived variability in chlorophyll, wind
1442 stress, sea surface height, and temperature in the northern California Current system,
1443 *J. Geophys. Res.*, *113*, C03015, doi:10.1029/2007JC004481.

1444 Ware, D. M., and R. E. Thomson (2005), Bottom-up ecosystem trophic dynamics
1445 determine fish production in the Northeast Pacific, *Science*, *308*(5726), 1280–1284,
1446 doi:10.1126/science.1109049.
1447
1448 Warner, J. C., W. R. Geyer, and J. A. Lerczak (2005), Numerical modeling of an estuary:
1449 a comprehensive skill assessment, *J. Geophys. Res.*, *110*, C05001,
1450 doi:10.1029/2004JC002691.
1451
1452 Wiseman, W. J., and R. W. Garvine (1995), Plumes and coastal currents near large river
1453 mouths, *Estuaries Coasts*, *18*(3), 509–517.
1454 Wolter, K., and M. S. Timlin (1993), Monitoring ENSO in COADS with a seasonally
1455 adjusted principal component index. *Proc. of the 17th Climate Diagnostics*
1456 *Workshop*, NOAA/N MC/CAC, NSSL, Oklahoma Climate Survey, CIMMS and the
1457 School of Meteor., Univ. of Oklahoma, Norman, OK, pp. 52–57.
1458 Yankovsky, A. E., B. M. Hickey, and A. K. Munchow (2001), Impact of variable inflow
1459 on the dynamics of a coastal buoyant plume, *J. Geophys Res.*, *106*, 19809–19824.
1460 Zhang, Y., A. M. Baptista, and E. P. Myers (2004), A cross-scale model for 3D baroclinic
1461 circulation in estuary-plume-shelf systems: I. Formulation and skill assessment. *Cont.*
1462 *Shelf Res.*, *24*(18), 2187–2214, doi:10.1016/j.csr.2004.07.021.
1463 Zhang, Y., and A. M. Baptista (2008), SELFE: A semi-implicit Eulerian-Lagrangian
1464 finite-element model for cross-scale ocean circulation, *Ocean Model.*, *21*(3–4), 71–
1465 96.

1466 Zhang, Y. J., A. M. Baptista, B. Hickey, B. C. Crump, D. Jay, M. Wilkin, and C. Seaton
1467 (2009), Daily forecasts of Columbia River plume circulation: A tale of spring/summer
1468 cruises, *J. Geophys. Res.* (this volume).

1469

1469

1469 Figure Captions

1470

1471 Figure 1. Left panel: Satellite-derived chlorophyll data (July 23, 2004) illustrating the
1472 typically observed higher chlorophyll in the Columbia plume as well as north of the river
1473 mouth (compared to south of the plume and river mouth). The image was obtained under
1474 strong upwelling conditions, with a well developed southwest-tending plume as well as
1475 remnants of a north-tending plume (Liu et al., 2009a). Alongshore chlorophyll patterns
1476 agree well with observations presented later in the paper (Fig. 7). Right panels: Satellite-
1477 derived chlorophyll and turbidity June 12, 2005 illustrating a well developed southwest-
1478 tending Columbia plume and a weaker north-tending plume. The image was obtained one
1479 day after model runs shown in Figure 10. Figures from Kudela Laboratory.

1480 Figure 2. Locations of all sampling transects, moored sensor arrays and wind buoys and
1481 CODAR ranges, plotted on a satellite-derived sea surface temperature image on June 21,
1482 2006. Regional physical features of interest are noted.

1483

1484 Figure 3. The Multivariate ENSO index (MEI) and the Pacific Decadal Oscillation (PDO)
1485 Index from 1950 to the present. The MEI is computed from the six main variables in the
1486 tropical Pacific (Wolter and Timlin, 1993). The PDO is defined as the leading principal
1487 component of North Pacific monthly sea surface temperature variability (poleward of
1488 20N for the 1900-93 period) (Mantua et al., 1997).

1489

1490 Figure 4a. Seasonal Columbia River discharge measured at Beaver Army terminal for
1491 2004, 2005 and 2006, along with average discharge from 1992–2007. RISE field studies
1492 are indicated with the colored bars parallel to the x-axis.
1493
1494 Figure 4b. Cumulative upwelling index (CUI) (Bakun, 1973) calculated from winds at
1495 NDBC Buoy 46029 for the upwelling seasons of 2004, 2005 and 2006, along with the
1496 average CUI 1992–2007. The location of the wind station is shown in Figure 2. RISE
1497 field studies are indicated with the colored bars parallel to the x-axis. The integration was
1498 started at the spring transition each year as defined by M. Kosro.
1499
1500 Figure 5. Proportion of copepod community types in zooplankton tows at a station 5 nm
1501 offshore on the Newport line (44°39.1'N, 124°10.6'W). Figure from Peterson Lab.
1502
1503 Figure 6. Alongshelf component (positive northward) of wind at Buoy 46029 and near
1504 surface current at mooring RN, north of the Columbia mouth (see location in Figure 2)
1505 for each of the RISE field seasons. The field studies are shown with shaded bars. Sections
1506 from the "cardinal" sampling sections offshore of Grays Harbor (G) and Cape Meares (C)
1507 are indicated with vertical lines. Satellite data used in this paper (Fig. 1) are indicated (S)
1508 along with times of model runs displayed in Figure 10 (M). Current data provided by
1509 Dever Lab.
1510
1511 Figure 7. Contoured sections of chlorophyll (a) in mg L^{-1} and nitrate (b) in µM along the
1512 RISE cardinal transects ~100 km north (GH) and south (CM) of the river mouth,

illustrating alongshore similarities and differences between the central Washington and northern Oregon coasts. In each cruise, the sections were sampled within 1–2 days of each other at the beginning and again at the end of the cruise. Stations are indicated with inverted triangles. Environmental settings are indicated in Figure 6 and the location of the Columbia River plume is indicated with the heavy gray contours (S = 31 psu). Chlorophyll values above 5 and above 10 mg L^{-1} are indicated with green and red shading, respectively; nitrate values below 1µM and between 25 and 30 µM are shaded blue and red, respectively. Data from Bruland (nitrate) and Kudela (chlorophyll regression).

Figure 8. a) The mean fraction of total chlorophyll greater than 20 µm versus distance offshore for the Washington (GH) and Oregon (CM) on cardinal lines during 2005-2006. Location of the Columbia plume is shown in Figures 7a,b. Figure from Kudela Lab.

b) The mean fraction of total chlorophyll greater than 20 µm versus salinity for the Washington (GH) and Oregon (CM) lines during the June 2005 RISE cruise. Figure from Kudela Lab.

Figure 9. Maximal chlorophyll-normalized productivity (P^B_m) as a function of percent transmission (beam transmissometer; 660 nm) for stations from the river plume during August 2005. Similar trends were obtained for other years. Photosynthesis-irradiance curve data were obtained as described by Kudela et al. (2006).

Figure 10. Comparison of surface salinity from two models of the Columbia plume: ROMS (MacCready et al., 2009) on the left and SELFE (Burla et al., 2009) on the right during (a) a downwelling wind period and (b) an upwelling wind period. The white

contour is the 200 m isobath. Model comparison dates are shown in Figure 6. On the right hand side of each figure sections from the models are compared with each other and with data taken within 5 hours of the model output time. Model results are from MacCready and Baptista Labs; observations from Hickey Lab. A satellite-derived turbidity image obtained one day after the model maps in panel (b) is shown in Figure 1.

Figure 11. Structure of the tidal plume and turbulent dissipation as revealed through 120 kHz acoustic backscatter (top; warm colors indicate scattering from turbulence and biology) and ADCP-derived horizontal velocity (bottom). Acoustic backscatter (upper panel), shear squared (middle panel) and along-axis velocity (lower panel) during a moderate ebb plume in August 8, 2005. Gray bars in the bottom panel show turbulent dissipation rate. Distances are referenced to the river's mouth to the east. This transect was taken along 46^{o} 14.4 N. These figures capture lift-off of the tidal plume from the bottom near x = -7.8 km; transition from strongly-sheared to layered flow near 11.5 km; and its culmination into a 20-m deep, convergent and highly-turbulent front propagating to the west as a gravity current at 1 ms^{-1} near x = -14 km. Adapted from Kilcher (2008).

Figure 12. A working model of the processes controlling supply, mixing and fate of nutrients, phytoplankton and salt in the vicinity of the Columbia River plume. The age of plume water is color coded (see key). In general, iron, phytoplankton and nitrate fluxes or pathways are indicated with red, green and blue arrows, respectively. Black curved arrows indicate mixing; red, single arrows indicate iron flux; green arrows indicate phytoplankton fluxes (single arrow, one way fluxes; double arrow, two way fluxes); the green or blue tracks with arrowheads indicate transport of biomass; black arrows indicate flow.

Table 1. RISE Program Elements

Component	**Techniques**	**Team Leaders**
Management and Synthesis		Hickey
Physical Modeling	Numerical models, ROMS and SELFE with MM5 forcing, NCOM boundaries	MacCready, Baptista
Biophysical Modeling	3D Numerical models	Banas
Water Properties, underway and CTD	Underway and CTD	Hickey, Jay, Kudela
Water Properties	TRIAXUS tow-fish	Jay
Water Properties	Moored arrays	Dever
Suspended particulate and size concentration	LISST-FLOC. acoustic backscatter	Jay, Horner-Devine
Chlorophyll a and phaeopigments	In vivo and in vitro Fluorometry	Kudela
Dissolved Nutrients including trace metals	Surveys and towed fish, Lachat autoanalyzer Flow injection, voltammetry, extraction/ICP-MS	Bruland
Picoplankton	FCM	Kudela, Lessard
Autotrophic/Heterotrophic nano/microplankton	FlowCAM, microscopy/image analysis	Lessard
Nitrogen Uptake	15N nitrogen kinetics	Kudela
Phytoplankton Growth and Microzooplankton Grazing Rates	Dilution method – size-fractionated chlorophyll a	Lessard, Kudela

	FlowCAM, microscopy	
Macrozooplankton Species and Abundance, Growth & Grazing	Net tows, Laser Optical Plankton Counter (LOPC), microscopy	Peterson
Hydrology	WWW data	Jay
Currents	Moorings, ADCP Surveys	Dever, Jay
Mixing Rates, Nutrient Fluxes	Profiles	Nash, Moum
Surface Eulerian Currents	CODAR, up to 180 km	Kosro
Lagrangian Currents	GPS drifters (with C,T)	Hickey
Remote Sensing,	AVHRR, SeaWiFS, MODIS, Bio-Optical modeling	Kudela
Remote Sensing of Fronts, Convergence	Synthetic Aperture Radar (SAR)	Jay

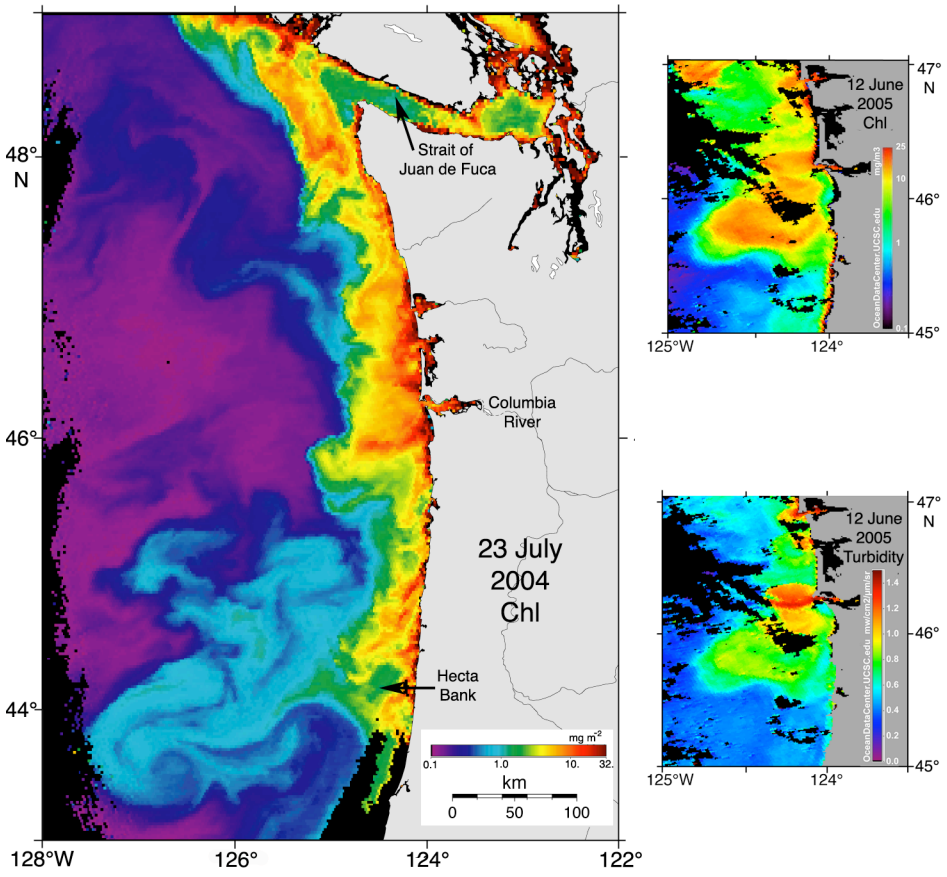
Strait of
Juan de Fuca
Columbia
River
23 July
2004
Chl
Hecta
Bank
mg m-2
0.1
1.0
10.
32.
km
0
50
100
48°
N
46°
44°
128°W
126°
124°
122°
12 June
2005
Chl
47°
N
46°
45°
125°W
124°
12 June
2005
Turbidity
47°
N
46°
45°
125°W
124°

Figure 1

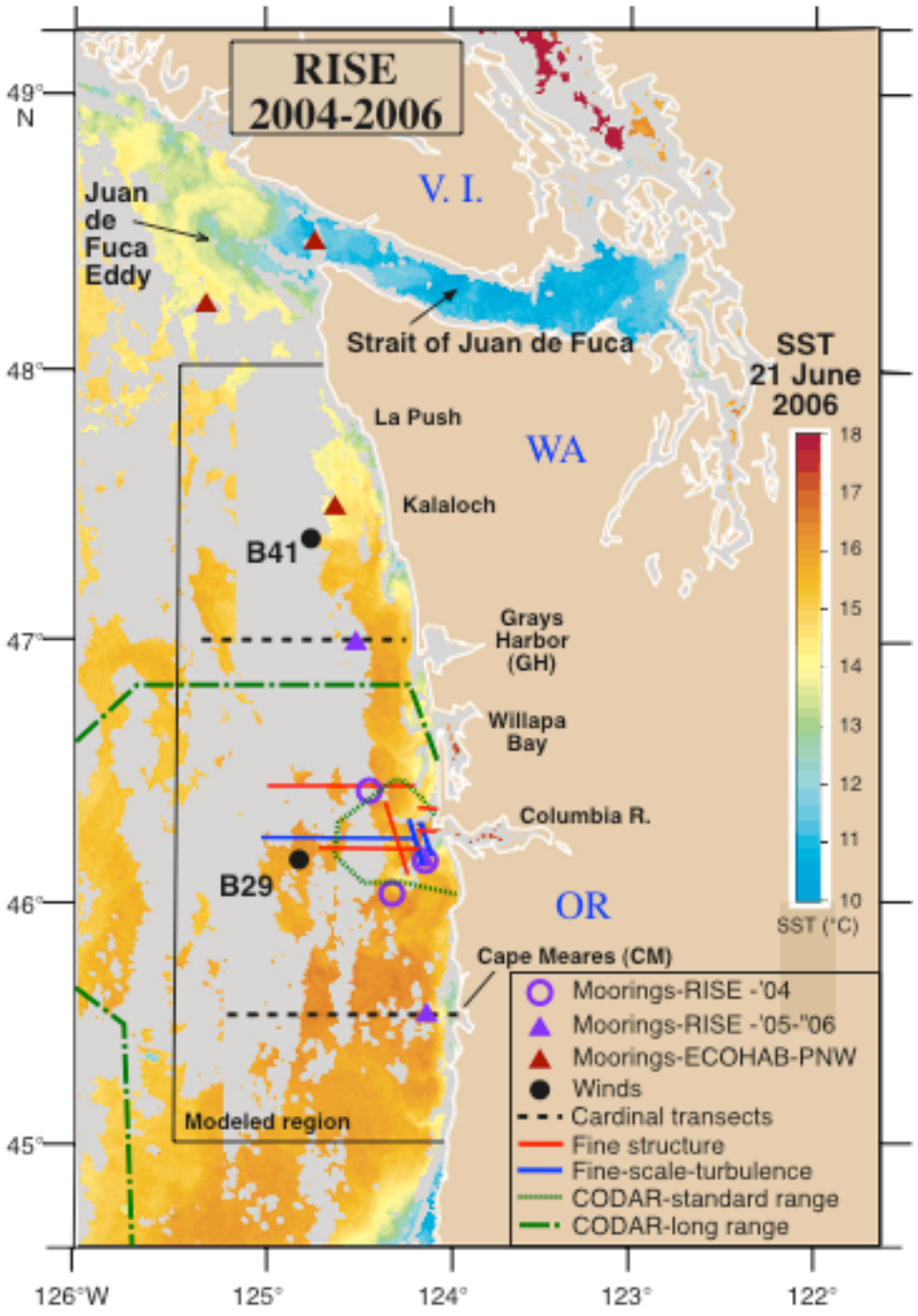
RISE
2004-2006
V. I.
Juan
de
Fuca
Eddy
Strait of Juan de Fuca
SST
21 June
2006
La Push
WA
Kalaloch
B41
Grays
Harbor
(GH)
Willapa
Bay
Columbia R.
B29
OR
Cape Meares (CM)
Modeled region
SST (°C)
18
17
16
15
14
13
12
11
10
49°
N
48°
47°
46°
45°
126°W
125°
124°
123°
122°
Moorings-RISE -'04
Moorings-RISE -'05-"06
Moorings-ECOHAB-PNW
Winds
Cardinal transects
Fine structure
Fine-scale-turbulence
CODAR-standard range
CODAR-long range

Figure 2

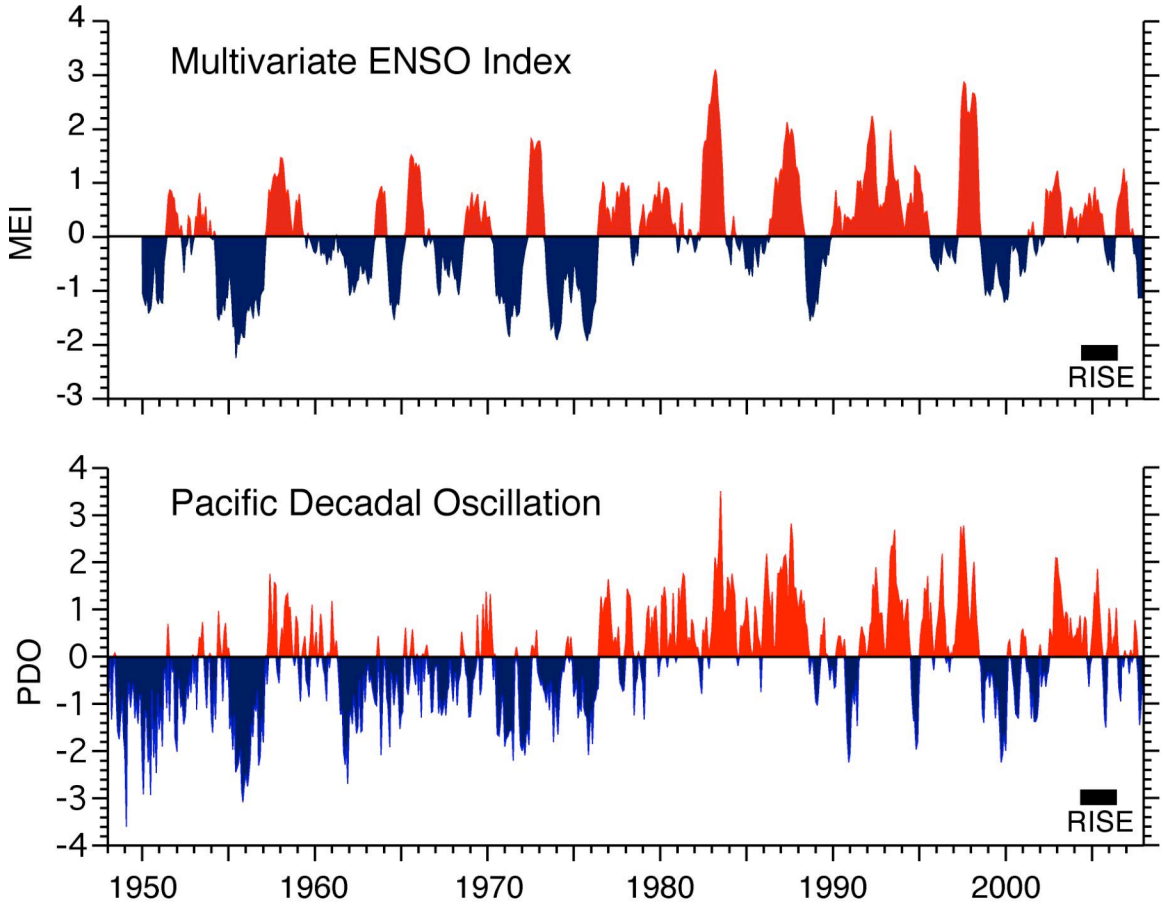
Multivariate ENSO Index
MEI
RISE
Pacific Decadal Oscillation
PDO
RISE
4
3
2
1
0
-1
-2
-3
-4
1950
1960
1970
1980
1990
2000

Figure 3

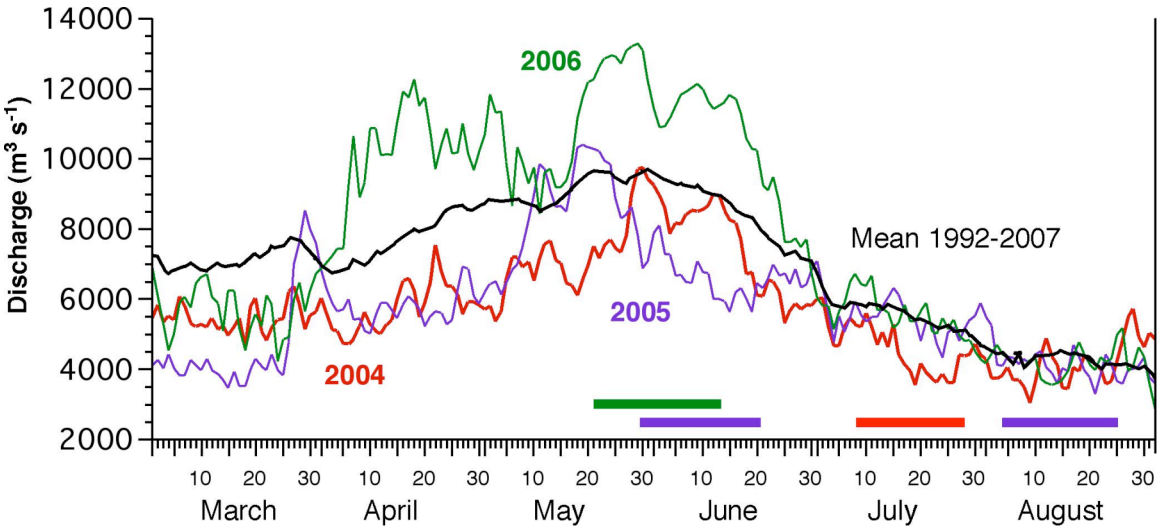

Figure 4a

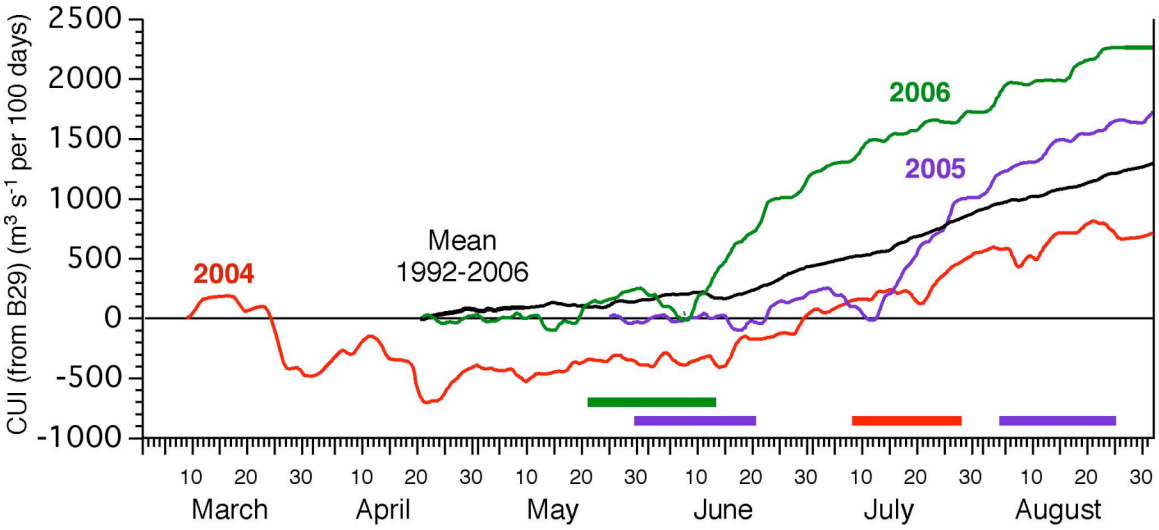

Figure 4b

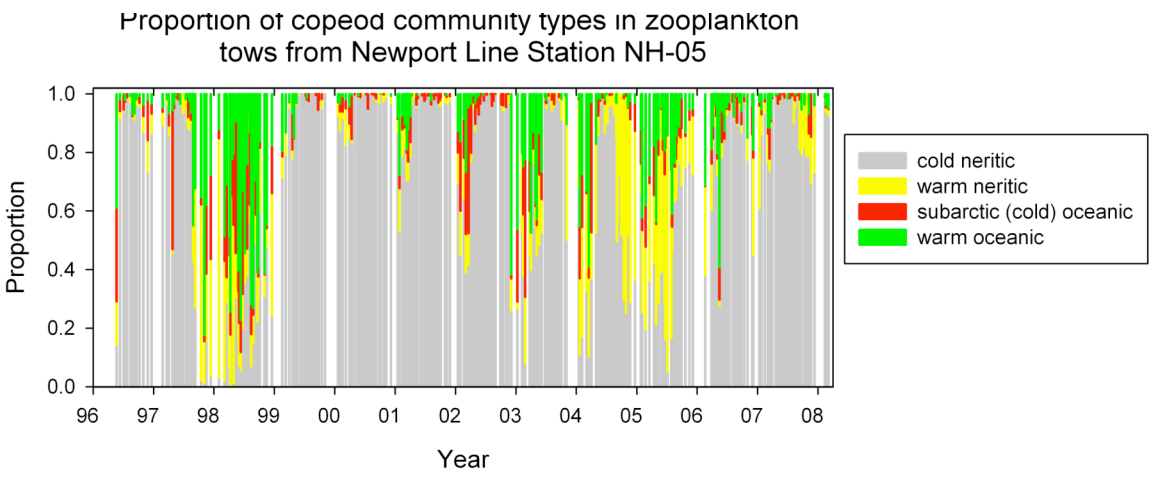
Proportion of copeod community types in zooplankton tows from Newport Line Station NH-05
Proportion
1.0
0.8
0.6
0.4
0.2
0.0
96
97
98
99
00
01
02
03
04
05
06
07
08
Year
cold neritic
warm neritic
subarctic (cold) oceanic
warm oceanic

Figure 5

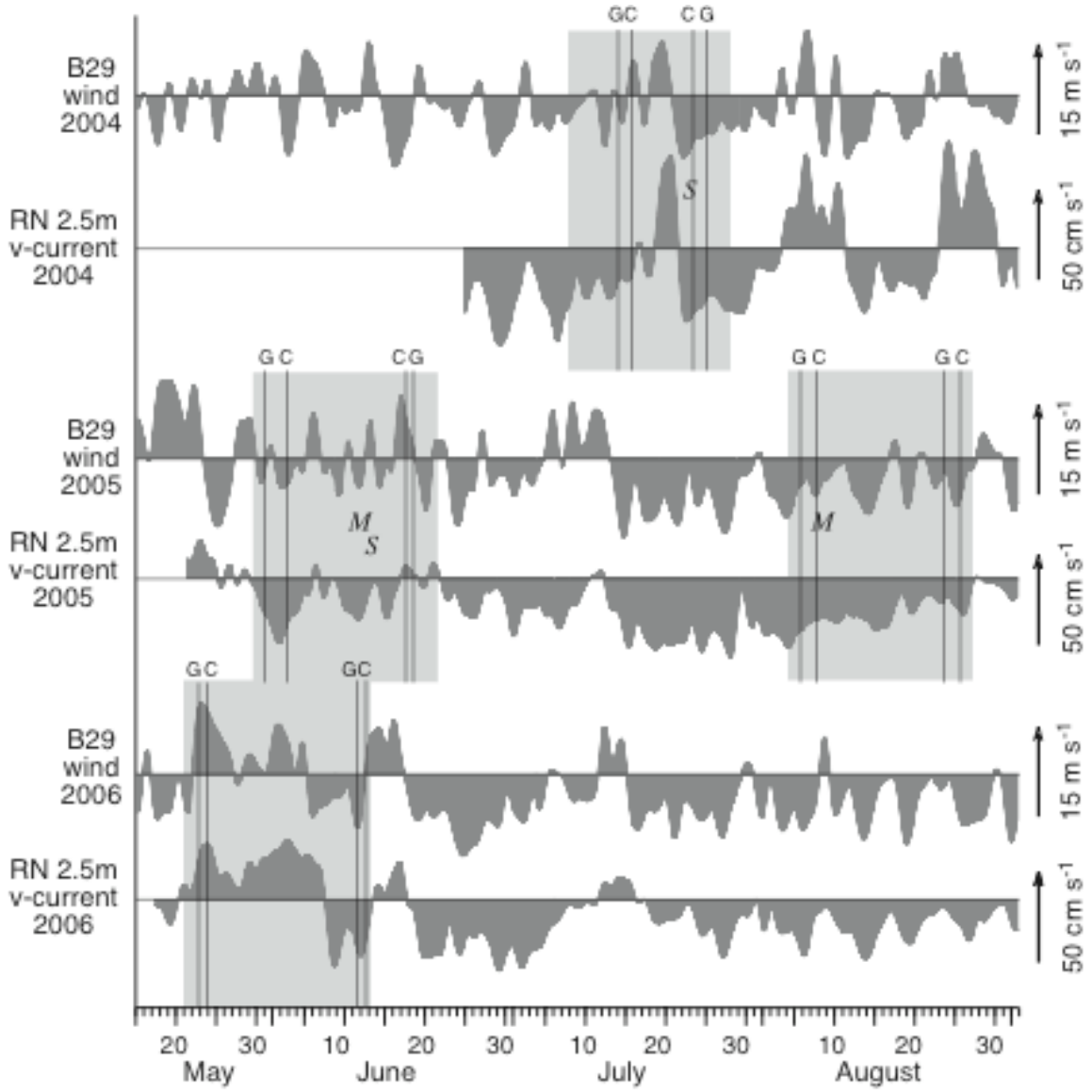
GC
CG
B29
wind
2004
15 m s-1
S
RN 2.5m
v-current
2004
50 cm s-1
GC
CG
GC
GC
B29
wind
2005
15 m s-1
M
S
M
RN 2.5m
v-current
2005
50 cm s-1
GC
GC
B29
wind
2006
15 m s-1
RN 2.5m
v-current
2006
50 cm s-1
20
30
10
20
30
10
20
30
10
20
30
May
June
July
August

Figure 6

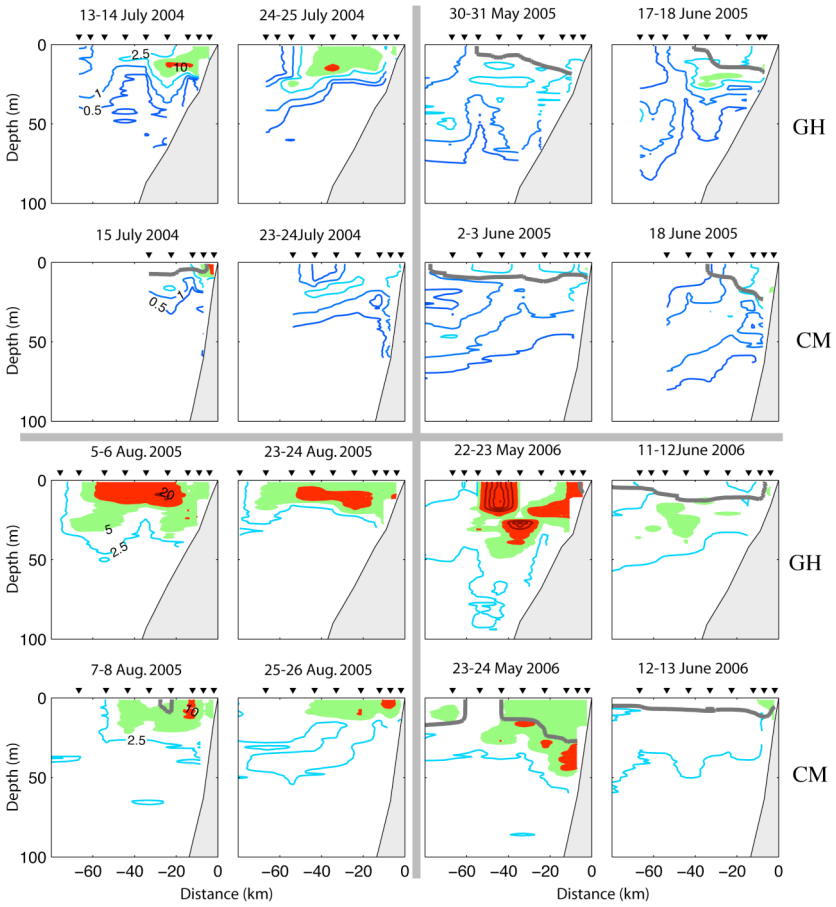
13-14 July 2004
24-25 July 2004
30-31 May 2005
17-18 June 2005
GH
15 July 2004
23-24July 2004
2-3 June 2005
18 June 2005
CM
5-6 Aug. 2005
23-24 Aug. 2005
22-23 May 2006
11-12June 2006
GH
7-8 Aug. 2005
25-26 Aug. 2005
23-24 May 2006
12-13 June 2006
CM
Depth (m)
0
50
100
−60 −40 −20 0
Distance (km)

Figure 7a

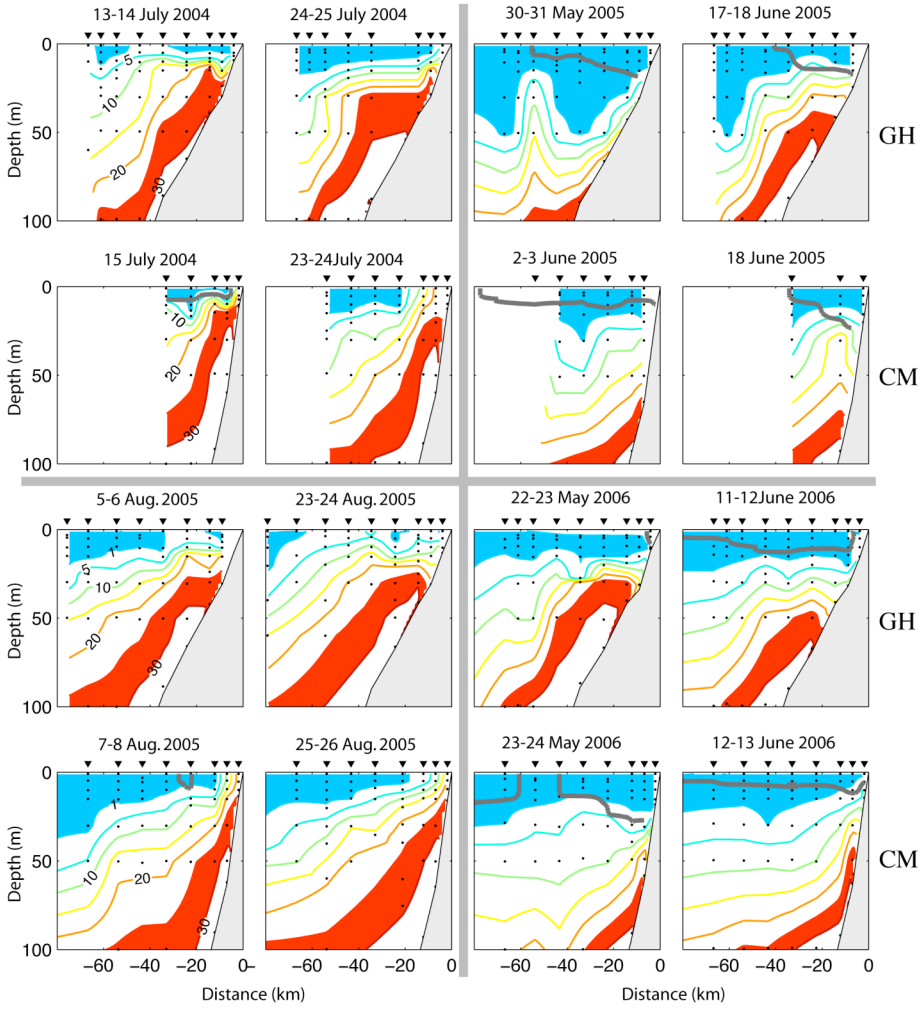
13-14 July 2004
24-25 July 2004
30-31 May 2005
17-18 June 2005
GH
15 July 2004
23-24July 2004
2-3 June 2005
18 June 2005
CM
5-6 Aug. 2005
23-24 Aug. 2005
22-23 May 2006
11-12June 2006
GH
7-8 Aug. 2005
25-26 Aug. 2005
23-24 May 2006
12-13 June 2006
CM
Depth (m)
0
50
100
5
10
20
30
−60
−40
−20
0
Distance (km)

Figure 7b

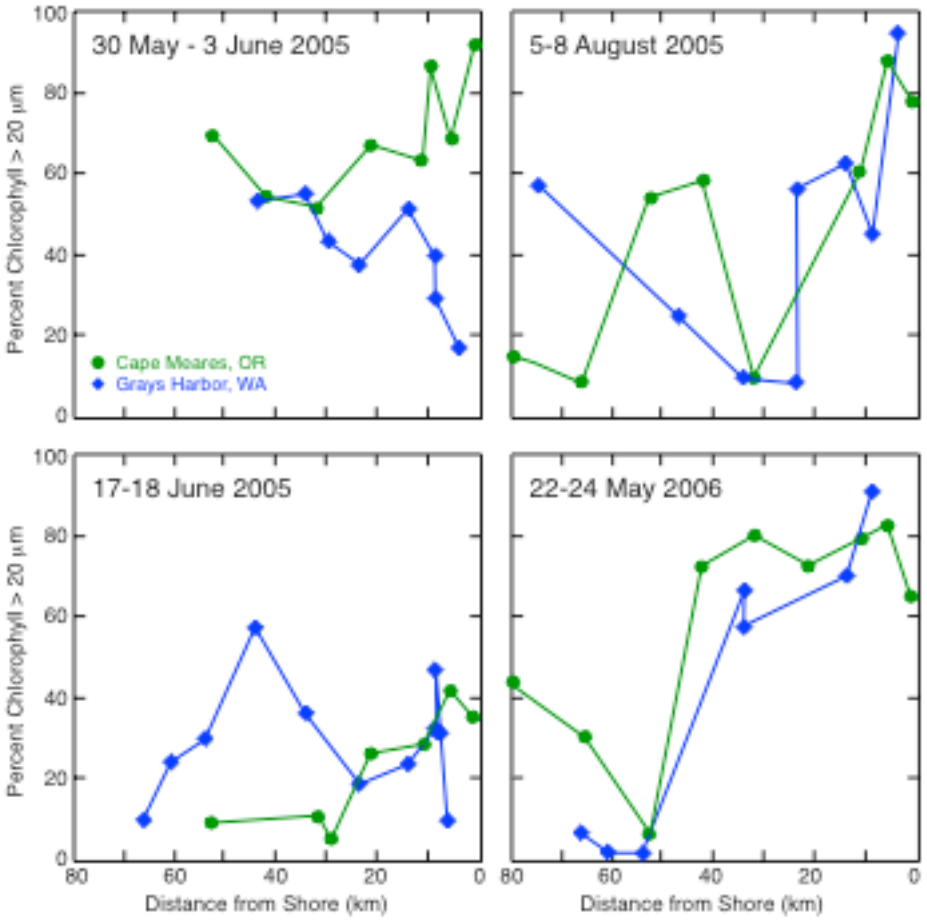
30 May - 3 June 2005
5-8 August 2005
17-18 June 2005
22-24 May 2006
Cape Meares, OR
Grays Harbor, WA
Percent Chlorophyll > 20 µm
Distance from Shore (km)
0
20
40
60
80
100

Figure 8a

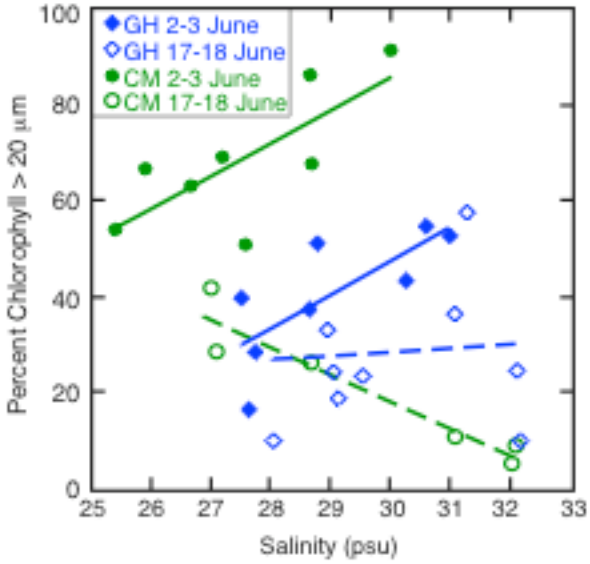
GH 2-3 June
GH 17-18 June
CM 2-3 June
CM 17-18 June
Percent Chlorophyll > 20 µm
Salinity (psu)
0
20
40
60
80
100
25
26
27
28
29
30
31
32
33

Figure 8b

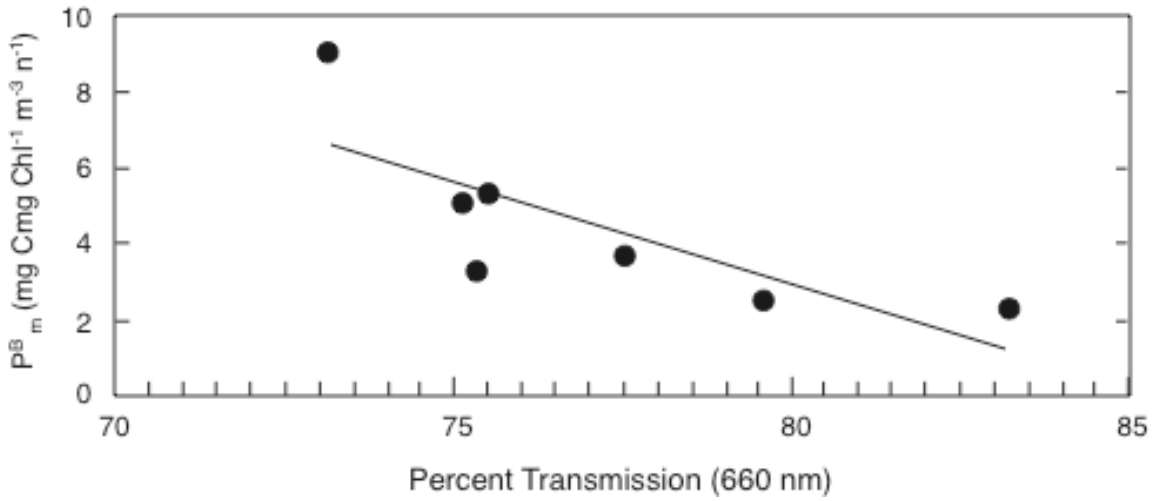
10
8
6
4
2
0
70
75
80
85
P^B_m (mg Cmg Chl^{-1} m^{-3} n^{-1})
Percent Transmission (660 nm)

Figure 9

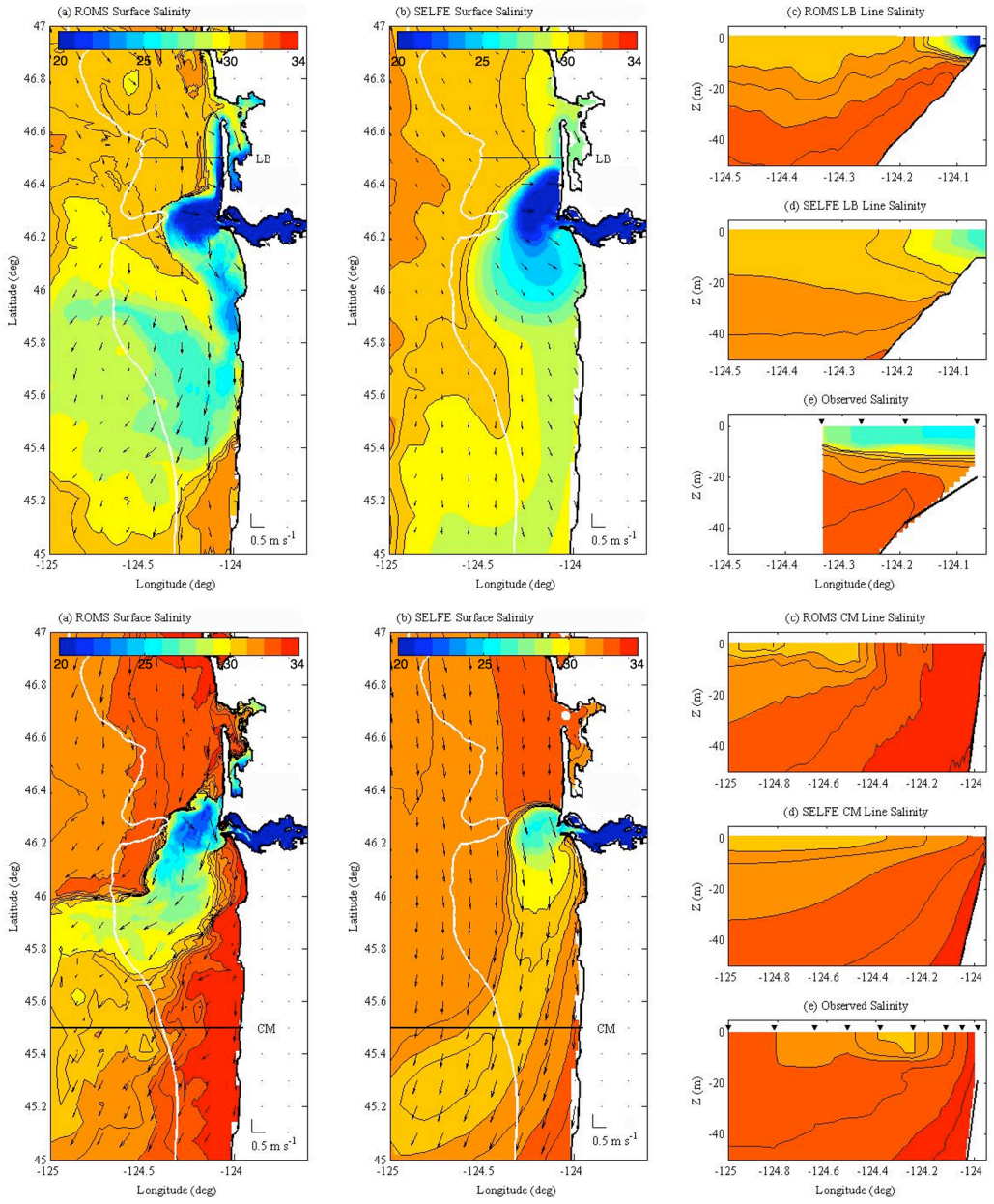
(a) ROMS Surface Salinity
(b) SELFE Surface Salinity
(c) ROMS LB Line Salinity
(d) SELFE LB Line Salinity
(e) Observed Salinity
LB
0.5 m s-1
Latitude (deg)
Longitude (deg)
Z (m)
(a) ROMS Surface Salinity
(b) SELFE Surface Salinity
(c) ROMS CM Line Salinity
(d) SELFE CM Line Salinity
(e) Observed Salinity
CM
0.5 m s-1
Latitude (deg)
Longitude (deg)
Z (m)

Figure 10

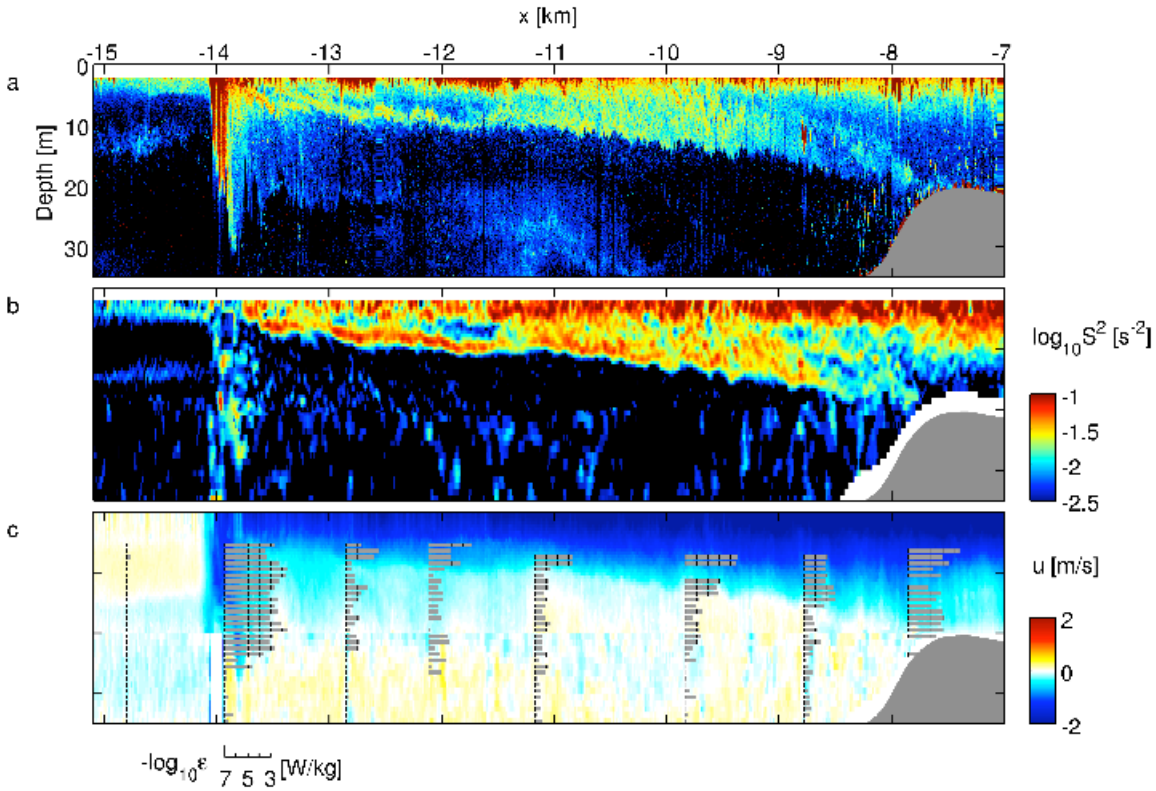
x [km]
-15
-14
-13
-12
-11
-10
-9
-8
-7
a
Depth [m]
0
10
20
30
b
log10S2 [s-2]
-1
-1.5
-2
-2.5
c
u [m/s]
2
0
-2
-log10ε
7 5 3 [W/kg]

Figure 11

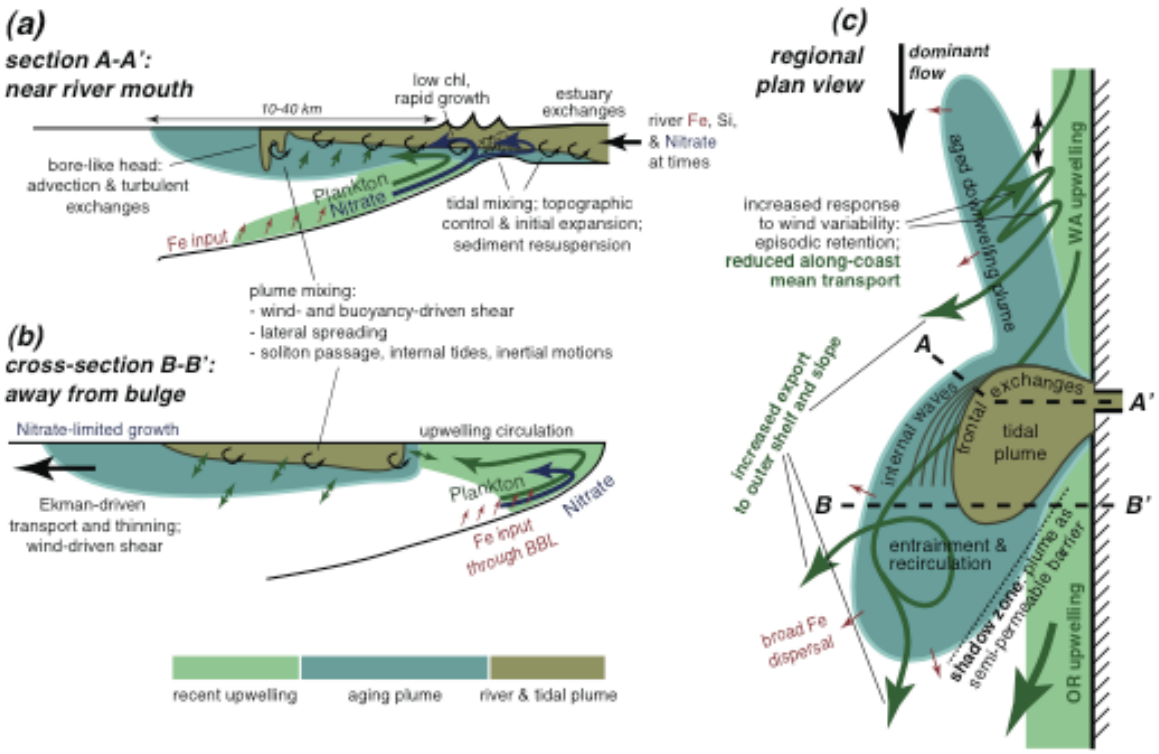
(a)
section A-A':
near river mouth
10-40 km
low chl,
rapid growth
estuary
exchanges
river Fe, Si,
& Nitrate
at times
bore-like head:
advection & turbulent
exchanges
Plankton
Nitrate
Fe input
tidal mixing; topographic
control & initial expansion;
sediment resuspension
plume mixing:
- wind- and buoyancy-driven shear
- lateral spreading
- soliton passage, internal tides, inertial motions
(b)
cross-section B-B':
away from bulge
Nitrate-limited growth
upwelling circulation
Ekman-driven
transport and thinning;
wind-driven shear
Plankton
Nitrate
Fe input
through BBL
recent upwelling
aging plume
river & tidal plume
(c)
regional
plan view
dominant
flow
aged downwelling plume
WA upwelling
increased response
to wind variability:
episodic retention;
reduced along-coast
mean transport
increased export
to outer shelf and slope
A
A'
internal waves
frontal exchanges
tidal
plume
B
B'
entrainment &
recirculation
broad Fe
dispersal
shadow zone: plume as
semi-permeable barrier
OR upwelling

Figure 12